through constitutive oligomerization, as has been suggested for the EGF receptor, or via induction of a conformational change, as reported with CD16. Notably, polymorphic S128R-E-selectin exhibited constitutive phosphorylation of ERK1/2 and p38 MAPK without leukocyte adhesion, which indicates that a potential conformational change of E-selectin attributable to the S128R polymorphism may influence the intracellular signaling pathway of E-selectin. The presence of soluble ligands in the assay medium can be neglected, because an enhanced phosphorylation of ERK kinase was observed in the absence of serum in the media (data not shown). A chemical cross-linking approach for potential oligomerization of E-selectin failed to show the difference between WT- and S128R-E-selectin–transduced HUVECs (data not shown); therefore, the responsible mechanisms underlying the altered MAPK signaling pathway observed with S128R mutant E-selectin seem to involve complex processes, which we hope to focus on in a future project.

The participation of the ERK1/2 signaling pathway in E-selectin–dependent PMN adhesion to vascular endothelium was recently identified.[18] Thus, the constitutive activation of ERK1/2 and p38 MAPK observed with S128R-E–transduced HUVECs may be a result of dysregulation of the E-selectin–dependent signaling in endothelial cells, which may play a role in the pathogenesis of MI. We have begun a series of experiments to elucidate the detailed molecular mechanisms involved in the constitutive phosphorylation of MAPKs.

Additional study of the pathological consequences of these disease-associated polymorphisms may provide a significant contribution to understanding the mechanisms of atherosclerosis as well as provide future diagnostic approaches to cardiovascular diseases.

## Acknowledgments

This work was supported by Special Coordination Funds and a grant-in-aid for Scientific Research on Priority Areas (C) of "Medical Genome Science" from the Ministry of Education, Culture, Sports, Science and Technology of Japan. The authors wish to thank Yoshie Nakamura for her technical assistance.

## References

1. Ross R. Atherosclerosis: an inflammatory disease. *N Engl J Med.* 1999; 340:115–126.
2. Bevilacqua MP, Nelson RM, Mannori G, Cecconi O. Endothelial-leukocyte adhesion molecules in human disease. *Annu Rev Med.* 1994; 45:361–378.
3. Bevilacqua MP, Nelson RM. Selectins. *J Clin Invest.* 1993;91:379–387.
4. Milstone DS, Fukumura D, Padgett RC, O'Donnell PE, Davis VM, Benavidez OJ, Monsky WL, Melder RJ, Jain RK, Gimbrone MA Jr. Mice lacking E-selectin show normal numbers of rolling leukocytes but reduced leukocyte stable arrest on cytokine-activated microvascular endothelium. *Microcirculation.* 1998;5:153–171.
5. Wenzel K, Ernst M, Rohde K, Baumann G, Speer A. DNA polymorphisms in adhesion molecule genes: a new risk factor for early atherosclerosis. *Hum Genet.* 1996;97:15–20.
6. Ye SQ, Usher D, Virgil D, Zhang LQ, Yochim SE, Gupta R. A PstI polymorphism detects the mutation of serine128 to arginine in CD 62E gene: a risk factor for coronary artery disease. *J Biomed Sci.* 1999;6: 18–21.
7. Wenzel K, Felix S, Kleber FX, Brachold R, Menke T, Schattke S, Schulte KL, Glaser C, Rohde K, Baumann G, Speer A. E-selectin polymorphism and atherosclerosis: an association study. *Hum Mol Genet.* 1994;3: 1935–1937.
8. Revelle BM, Scott D, Beck PJ. Single amino acid residues in the E- and P-selectin epidermal growth factor domains can determine carbohydrate binding specificity. *J Biol Chem.* 1996;271:16160–16170.
9. Yoshida M, Szente BE, Kiely JM, Rosenzweig A, Gimbrone MA Jr. Phosphorylation of the cytoplasmic domain of E-selectin is regulated during leukocyte-endothelial adhesion. *J Immunol.* 1998;161:933–941.
10. Ishii H, Yoshida M, Rosenzweig A, Gimbrone MA Jr, Yasukochi Y, Numano F. Adenoviral transduction of human E-selectin into isolated, perfused, rat aortic segments: an ex vivo model for studying leukocyte-endothelial interactions. *J Leukoc Biol.* 2000;68:687–692.
11. Gerszten RE, Garcia-Zepeda EA, Lim YC, Yoshida M, Ding HA, Gimbrone MA Jr, Luster AD, Luscinskas FW, Rosenzweig A. MCP-1 and IL-8 trigger firm adhesion of monocytes to vascular endothelium under flow conditions. *Nature.* 1999;398:718–723.
12. Rodriguez-Romero A, Almog O, Tordova M, Randhawa Z, Gilliland GL. Primary and tertiary structures of the Fab fragment of a monoclonal anti-E-selectin 7A9 antibody that inhibits neutrophil attachment to endothelial cells. *J Biol Chem.* 1998;273:11770–11775.
13. Bevilacqua MP, Stengelin S, Gimbrone MA Jr, Seed B. Endothelial leukocyte adhesion molecule 1: an inducible receptor for neutrophils related to complement regulatory proteins and lectins. *Science.* 1989;243: 1160–1165.
14. Luscinskas FW, Kansas GS, Ding H, Pizcueta P, Schleiffenbaum BE, Tedder TF, Gimbrone M Jr. Monocyte rolling, arrest and spreading on IL-4-activated vascular endothelium under flow is mediated via sequential action of L-selectin, $\beta_1$-integrins, and $\beta_2$-integrins. *J Cell Biol.* 1994;125:1417–1427.
15. Gerszten RE, Luscinskas FW, Ding HT, Dichek DA, Stoolman LM, Gimbrone M Jr, Rosenzweig A. Adhesion of memory lymphocytes to vascular cell adhesion molecule-1–transduced human vascular endothelial cells under simulated physiological flow conditions in vitro. *Circ Res.* 1996;79:1205–1215.
16. Wenzel K, Stahn R, Speer A, Denner K, Glaser C, Affeldt M, Moobed M, Scheer A, Baumann G, Felix SB. Functional characterization of atherosclerosis-associated Ser128Arg and Leu554Phe E-selectin mutations. *Biol Chem.* 1999;380:661–667.
17. Yoshida M, Westlin WF, Wang N, Ingber DE, Rosenzweig A, Resnick N, Gimbrone MA Jr. Leukocyte adhesion to vascular endothelium induces E-selectin linkage to the actin cytoskeleton. *J Cell Biol.* 1996;133: 445–455.
18. Hu Y, Kiely JM, Szente BE, Rosenzweig A, Gimbrone MA Jr. E-Selectin-dependent signaling via the mitogen-activated protein kinase pathway in vascular endothelial cells. *J Immunol.* 2000;165:2142–2148.
19. Herrmann SM, Ricard S, Nicaud V, Mallet C, Evans A, Ruidavets JB, Arveiler D, Luc G, Cambien F. The P-selectin gene is highly polymorphic: reduced frequency of the Pro715 allele carriers in patients with myocardial infarction. *Hum Mol Genet.* 1998;7:1277–1284.
20. Ellsworth DL, Bielak LF, Turner ST, Sheedy IP, Boerwinkle E, Peyser PA. Gender- and age-dependent relationships between the E-selectin S128R polymorphism and coronary artery calcification. *J Mol Med.* 2001;79:390–398.
21. Sasaoka T, Kimura A, Hohta SA, Fukuda N, Kurosawa T, Izumi T. Polymorphisms in the platelet-endothelial cell adhesion molecule-1 (PECAM-1) gene, Asn563Ser and Gly670Arg, associated with myocardial infarction in the Japanese. *Ann N Y Acad Sci.* 2001;947: 259–269.
22. Fernandes H, Cohen S, Bishayee S. Glycosylation-induced conformational modification positively regulates receptor-receptor association: a study with an aberrant epidermal growth factor receptor (EGFRvIII/DeltaEGFR) expressed in cancer cells. *J Biol Chem.* 2001;276: 5375–5383.
23. Freeburn RW, Gale RE, Linch DC. Activating point mutations in the $\beta$C chain of the GM-CSF, IL-3 and IL-5 receptors are not a major contributory factor in the pathogenesis of acute myeloid leukaemia. *Br J Haematol.* 1998;103:66–71.

# Amlodipine Modulates THP-1 Cell Adhesion to Vascular Endothelium via Inhibition of Protein Kinase C Signal Transduction

Tao Yu, Ikuo Morita, Kentaro Shimokado, Takehisa Iwai, Masayuki Yoshida

*Abstract*—Inflammatory responses play an important role in atherosclerosis. To critically assess the effect of dihydropyridines in inflammatory reactions, we conducted a monocyte-endothelial adhesion assay with monocytic THP-1 cells treated with amlodipine under flow conditions in vitro. THP-1 cells were incubated in the presence of amlodipine (10 μmol/L) for 48 hours and then perfused over activated (interleukin-1β, 10 U/mL, 4 hours) human umbilical vein endothelial cells. The adhesion of THP-1 cells was significantly reduced after amlodipine treatment ($P<0.001$); however, flow cytometric analysis reveled that the expression levels of integrins in THP-1 cells were not significantly altered. Furthermore, Western blotting analysis of THP-1 cell lysates revealed that translocation of RhoA from the cytosol to the membrane was significantly diminished after amlodipine treatment. In addition, activation of protein kinase C-α and -β, as well as intracellular calcium influx, induced by phorbol 12-myristate 13-acetate, was diminished after amlodipine treatment. Pretreatment of THP-1 cells with calphostin C, a potent inhibitor of protein kinase C, significantly reduced THP-1 adhesion to vascular endothelium, whereas activation of $\beta_1$-integrin was reduced after amlodipine treatment in THP-1 cells, based on the immunoreactivity of an activation-specific antibody for $\beta_1$-integrin. Similar inhibitory effects were observed when we used freshly isolated peripheral blood mononuclear cells. These findings suggest a potential role for amlodipine in monocyte-endothelial interactions by modulation of protein kinase C- and RhoA-dependent mechanisms, which might account for its vascular protective effects. (***Hypertension.* 2003;42: 329-334.)**

**Key Words:** calcium channel blockers ■ cell adhesion molecules ■ monocytes ■ protein kinases ■ signal transduction

L-type calcium channel antagonists are widely used in the management of hypertension as well as coronary heart diseases, and an increasing number of reports support the therapeutic benefits of these compounds for patients with cardiovascular diseases. Recently, amlodipine, a $Ca^{2+}$ channel blocker, was shown to reduce the progression of atherosclerotic plaque formation in rabbit models,[1,2] suggesting its role in atherosclerosis. In one of those studies, amlodipine caused a significant and dose-dependent reduction in lesion formation in the thoracic aorta,[1] whereas in another, it exhibited an atheroprotective effect by acting as an antioxidant and reducing LDL uptake by the vessel wall, which consequently limited the size and extent of lesional areas.[3] These two findings have been proposed to show potential mechanisms for the antiatherosclerotic effect of amlodipine. In addition to those findings, the results of several in vitro studies also indicate that treatment with amlodipine enhances nitric oxide production in endothelial cells,[4] suggesting an anti-inflammatory role for the compound. In the present study, we attempted to elucidate the molecular mechanism responsible for the anti-inflammatory role of amlodipine by using an in vitro flow-chamber apparatus to examine amlodipine's effect on monocyte-endothelial interaction. We found that amlodipine reduced the adhesion of THP-1 and human umbilical vein endothelial cells (HUVECs) and also inhibited protein kinase C (PKC) activation and RhoA translocation. Thus, our results provide concrete biologic evidence for the antiatherosclerotic potential of amlodipine.

## Methods

### Reagents and Cells

THP-1, a human leukemia cell line of monocyte/macrophage lineage, was obtained from American Type Culture Collection (Manassas, Va) and grown in RPMI-1640 medium with 10% fetal bovine serum. Peripheral blood mononuclear cells (PBMNCs) were isolated from whole blood drawn from healthy volunteers, as previously described.[5] HUVECs were isolated from normal-term umbilical cords as previously described.[6] All procedures involving human samples were conducted according to the Guidelines for Animal and Human Experimentation of Tokyo Medical and Dental University.

Received February 4, 2003; first decision February 27, 2003; revision accepted July 9, 2003.

From the Departments of Medical Biochemistry (T.Y., M.Y.), Vascular Surgery (T.Y., T.I.), Cellular Physiological Chemistry (I.M.), and Vascular Medicine (K.S., M.Y.), Graduate School of Medicine, Tokyo Medical and Dental University, Tokyo, Japan.

Correspondence to Masayuki Yoshida, MD, Department of Medical Biochemistry, Vascular Medicine, Graduate School of Medicine, Tokyo Medical and Dental University, 1-5-45, Yushima, Bldg D-256, Bunkyo-ku, Tokyo 113-8519, Japan, E-mail masavasc@tmd.ac.jp



*Hypertension* is available at http://www.hypertensionaha.org DOI: 10.1161/01.HYP.0000087199.34071.4F

For use in the flow-chamber apparatus, HUVECs (passages 2 and 3) were placed onto 22-mm, fibronectin-coated glass coverslips. The antibodies directed to the following molecules were used in the present study: CD11a (clone 38, Ancell Corp); CD11b (clone 44, YLEM); CD18 (clone MEM48, Southern Biotechnology Associates); CD49d (clone A4-PUJ1, Upstate Biotechnology); L-selectin (clone FMC46, Serotec); RhoA (Santa Cruz Biotechnology); $\beta_1$-integrin (clone HUTS21, PharMingen, and clone 4B7R, Santa Cruz Biotechnology); and PKC$\alpha$, -$\beta$, -$\delta$, and -$\iota$ (New England Biolabs). 4',6-diamidino-2-phenylindole (DAPI) and ionophore K23E1 were obtained from Dojindo Japan. Phorbol 12-myristate 13-acetate (PMA) was purchased from Wako Chemicals USA, Inc. Calphostin C was obtained from Calbiochem. Interleukin-1$\beta$ (IL-1$\beta$) was obtained from Genzyme. Dulbecco's phosphate-buffered saline (DPBS) was obtained from Sigma (D8662).

### Adhesion Assay Under Flow Conditions

We conducted an in vitro adhesion assay with monocytic THP-1 cells or PBMNCs treated with amlodipine under simulated flow conditions (estimated shear stress=1.0 dyn/cm$^2$) by using a protocol that has been previously described in detail.[6] THP-1 cells or PBMNCs were stained with a 0.25% trypan blue solution or a solution of DAPI (10 mmol/L Tris-HCl, pH 7.4, 10 mmol/L EDTA, 100 mmol/L NaCl, and 500 ng/mL DAPI) for 10 minutes at room temperature after incubation with amlodipine. THP-1 cells and PBMNCs ($10^5$ cells/mL) were diluted in the perfused medium (DPBS containing 0.2% human serum albumin) and then perfused over activated (IL-1$\beta$, 10 U/mL, 4 hours) HUVEC monolayers. The interactions of THP-1 cells or PBMNCs with HUVECs were observed under an inverted microscope (Olympus, IX70) and then analyzed by image analysis software. In some experiments, a static adhesion assay was performed as previously described.[5]

### Flow Cytometry

THP-1 cells were first incubated with the indicated primary antibodies on ice for 45 minutes, washed twice with RPMI-1640 medium containing 5% fetal calf serum, and then incubated with fluorescein isothiocyanate (FITC)–labeled goat anti-mouse antibody (1:50 dilution). Fluorescence intensity was analyzed with a fluorescence-activated cell sorting system (FACSCaliber, Becton-Dickinson).

### Translocation of RhoA and PKC in THP-1 Cells

The expression of RhoA and PKC was detected in the membrane and cytosol fractions of the THP-1 cell lysate by Western blotting as described previously.[6] An equal amount of protein (10 $\mu$g) from each fraction was subjected to 12.5% (RhoA) or 8% (PKC) sodium dodecyl sulfate–polyacrylamide gel electrophoresis, and Western blotting analysis was carried out with mouse monoclonal antibodies to RhoA and the indicated PKC isoforms.

### Quantification of Filamentous Actin in THP-1 Cells

Filamentous actin (F-actin) in THP-1 cells was quantitated as described previously.[6] In brief, THP-1 cells ($10^6$/mL) were fixed with 1% paraformaldehyde for 5 minutes, permeabilized with 0.1% Triton X-100 for 60 seconds, and incubated with FITC-conjugated phalloidin for 60 minutes. The fluorescence intensity of the THP-1 cells was quantified by using a fluorescence plate reader and was also observed under a fluorescence microscope.

### Calcium Concentration in THP-1 Cells

Next, we attempted to determine the effect of amlodipine on cytosolic calcium concentrations in THP-1 cells. THP-1 cells ($2\times10^6$ cells/mL) were preincubated in the presence or absence of amlodipine for 48 hours, washed with DPBS (1.2 mmol/L $Ca^{2+}$), and incubated in the dark at 37°C for 20 minutes in the presence of fura 2-AM (5 $\mu$g/mL). The cells were then washed and resuspended in DPBS at a density of $10^6$ cells/mL. To measure intracellular calcium ($[Ca^{2+}]_i$), 1 mL of the cell suspension was placed in the cuvette of a CAF-110 fluorescence spectrophotometer (Jasco Japan). PMA (10 ng/mL) was directly injected into the cuvette, and $[Ca^{2+}]_i$ was measured by excitation at 340 and 380 nm and fluorescence emission at 500 nm.

### Activity of $\beta_1$-Integrin in THP-1 Cells

The activity of $\beta_1$-integrin in THP-1 cells was examined by Western blotting analysis with the use of two independent monoclonal antibodies against human $\beta_1$-integrin (CD29), which were HUTS21 (recognizes an activation-dependent epitope) and 4B7R (recognizes activated and resting $\beta_1$-integrin), as described earlier.

### Statistical Analysis

Results are presented as mean±SD. Data were analyzed by ANOVA, with $P<0.05$ considered significant.

## Results

### Amlodipine Inhibits Adhesion of THP-1 Cells or PBMNCs to Activated HUVECs Under Flow Conditions

We examined the effect of amlodipine on monocyte-endothelial interactions under flow conditions (shear stress of 1.0 dyn/cm$^2$). When THP-1 cells or PBMNCs were incubated in the presence of amlodipine, the amount of adhesion to HUVECs (IL-1$\beta$, 10 U/mL, 4 hours) was decreased (Figure 1A). The inhibitory effect of amlodipine on THP-1 adhesion was statistically significant at a concentration of 10 $\mu$mol/L, compared with the control (amlodipine, 6.25±1.75/high-power field [HPF] vs control, 9.63±1.30/HPF; n=8, $P<0.001$), and similar effects were observed with PBMNCs (amlodipine, 7.11±1.76/HPF vs control, 12.78±1.86/HPF; n=8, $P<0.001$). These inhibitory effects were observed in a dose-dependent manner; however, they were not statistically significant with doses lower than 10 $\mu$mol/L (data not shown), and amlodipine treatment for <48 hours failed to exhibit a significant reduction of adhesion by THP-1 cells (data not shown). Furthermore, preliminary experiments with trypan blue and DAPI staining revealed that THP-1 cells were not dramatically damaged by amlodipine treatment up to a concentration of 10 $\mu$mol/L (data not shown). As a result, we chose to treat THP-1 cells with a concentration of 10 $\mu$mol/L for 48 hours, unless otherwise noted. On the other hand, when HUVECs were treated with amlodipine, no significant inhibitory effect was found in the adhesion assays (data not shown).

### Integrin Expression in THP-1 Cells

To elucidate the molecular mechanism of the observed inhibitory effect of amlodipine toward THP-1 cell adhesion, integrin expression levels were examined by flow cytometric analysis. THP-1 cells were incubated in the presence or absence of amlodipine (10 $\mu$mol/L, 48 hours); however, the expression levels of CD11a, CD11b, CD11c, CD18, and CD49d were not significantly different between the two conditions (Figure 1B).

### Amlodipine Reduces RhoA GTPase Activation in THP-1 Cells

We next examined the effects of amlodipine on the intracellular cytoskeleton networks in THP-1 cells. F-actin content was estimated by using fluorescently labeled phalloidin after treatment with amlodipine. As shown in Figure 2A, amlodip-

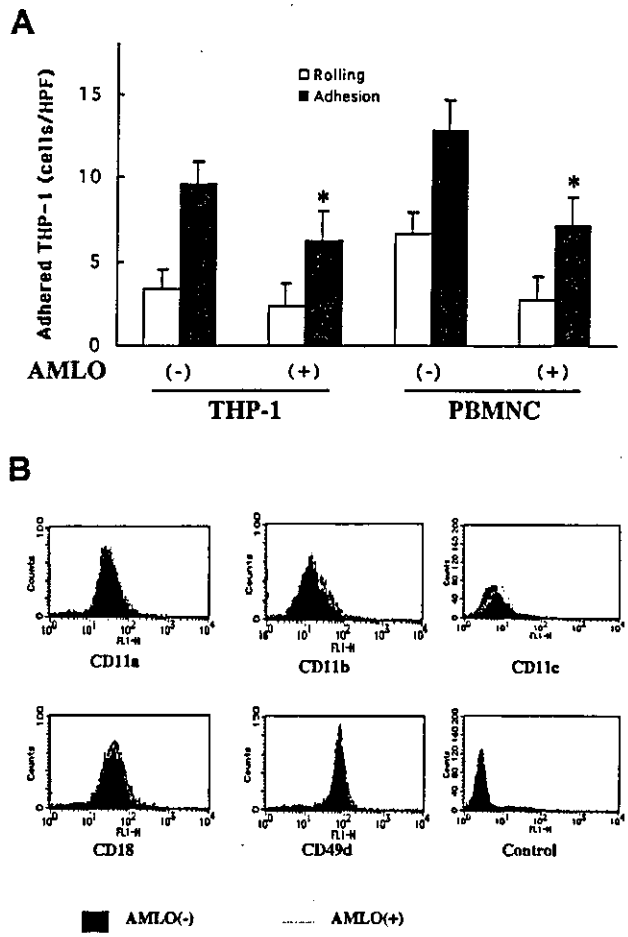


**Figure 1.** A, Effects of amlodipine (AMLO) on adhesion of THP-1 cells to HUVECs. THP-1 cells or PBMNCs ($2\times10^6$/mL) were incubated in the presence (+) or absence (−) of amlodipine for 48 hours and then perfused over HUVEC monolayers activated with 10 U/mL IL-1$\beta$ for 4 hours at a shear stress of 1.0 dyn/cm$^2$. Rolling and adherent THP-1 cells or PBMNCs on HUVEC monolayers were counted under 20× microscope fields for 10 minutes as described in Methods. Data are representative of 8 separate experiments. *$P$<0.001 vs amlodipine (−). B, Effects of amlodipine on integrin expression in THP-1 cells. THP-1 cells ($10^6$/mL) were incubated in the presence of 10 $\mu$mol/L amlodipine [AMLO(+)] or medium alone [AMLO(−)] for 48 hours. The expression levels of integrins in THP-1 cells were analyzed by flow cytometric analysis with monoclonal antibodies to CD11a, CD11b, CD11c, CD18, and CD49d for each condition. Five thousands cells were analyzed. Data are representative of 5 separate experiments.

ine treatment significantly reduced F-actin (amlodipine, 417.3±23.0 vs control, 564.8±4.8; $P$<0.001, n=6). Next, the activation of RhoA GTPase was also examined, because RhoA GTPase is regarded as crucial for cell motility and thus, for adhesive interactions.[7] Western blotting analysis revealed that the translocation of RhoA from the cytosol to the membrane was significantly decreased after incubation with amlodipine (10 $\mu$mol/L, 48 hours; Figure 2B).

## Amlodipine Reduces PKC Activation in THP-1 Cells

The involvement of PKC in amlodipine-dependent RhoA GTPase modulation was further investigated. To monitor

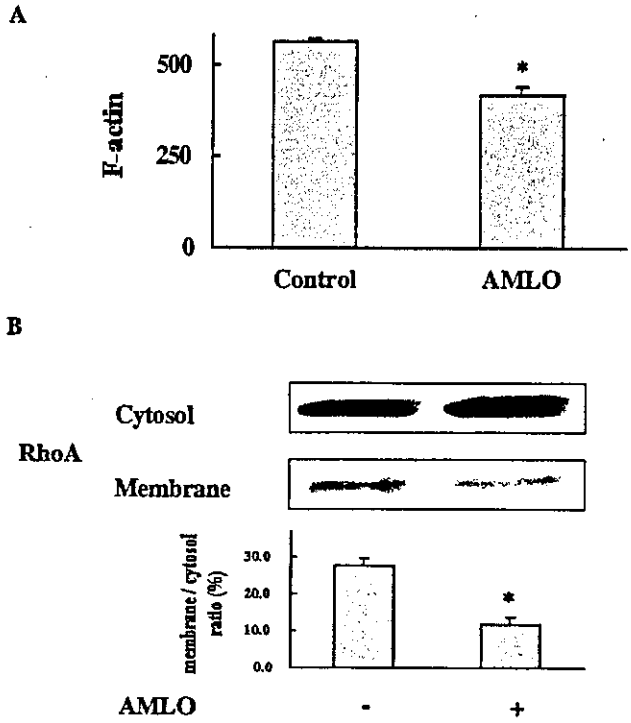


**Figure 2.** A, Effects of amlodipine on actin polymerization in THP-1 cells. THP-1 cells ($10^6$/mL) were incubated in the presence of 10 $\mu$mol/L amlodipine [AMLO(+)] or medium alone [AMLO(−)] for 48 hours. F-actin in THP-1 cells was detected with FITC-conjugated phalloidin, which was then observed under a fluorescence microscope, quantified with use of a fluorescence plate reader, and expressed as a percentage of control THP-1 cells. Data are representative of 6 separate experiments. *$P$<0.001 vs AMLO(−). B, Effects of amlodipine on RhoA GTPase activation in THP-1 cells. THP-1 cells ($10^6$/mL) were incubated in the presence of 10 $\mu$mol/L amlodipine [AMLO(+)] or medium alone [AMLO(−)] for 48 hours. RhoA expression was detected in membrane and cytosol lysates of THP-1 cells ($10^6$/mL) for each condition by Western blotting (10 $\mu$g protein/lane). Band densities were quantified by using an LAS1000 (FujiFilm) and are expressed in the bar graph shown. Blots are representative of 5 separate experiments. *$P$<0.001 vs AMLO(−).

PKC activation, the translocation of PKC from the cytosol to the membrane was examined.[8] Activation of PKC-$\alpha$ and PKC-$\beta$, as judged from their translocation into the membrane fraction, was observed in THP-1 cells after PMA stimulation; however, pretreatment with amlodipine significantly reduced this PMA-induced PKC activation (Figure 3A). Additional experiments revealed that the activated forms of other PKC isoforms, such as PKC-$\delta$and PKC-$\iota$, were not significantly reduced after pretreatment (data not shown).

To assess critically the involvement of the PKC-dependent mechanism in the adhesion of THP-1 to vascular endothelium, THP-1 cells were pretreated with 500 nmol/L calphostin C, a specific inhibitor of PKC,[9] for 30 minutes before the adhesion assays. As shown in Figure 3B, pretreatment with calphostin C reduced THP-1 adhesion to activated HUVECs, which was also observed with THP-1 cells treated with amlodipine, suggesting a primary role for PKC in this phenomenon. Furthermore, pretreatment with calphostin C inhibited the membrane translocation of RhoA induced by PMA, suggesting that PMA plays a role upstream of RhoA GTPase in controlling THP-1 adhesion (Figure 3C).

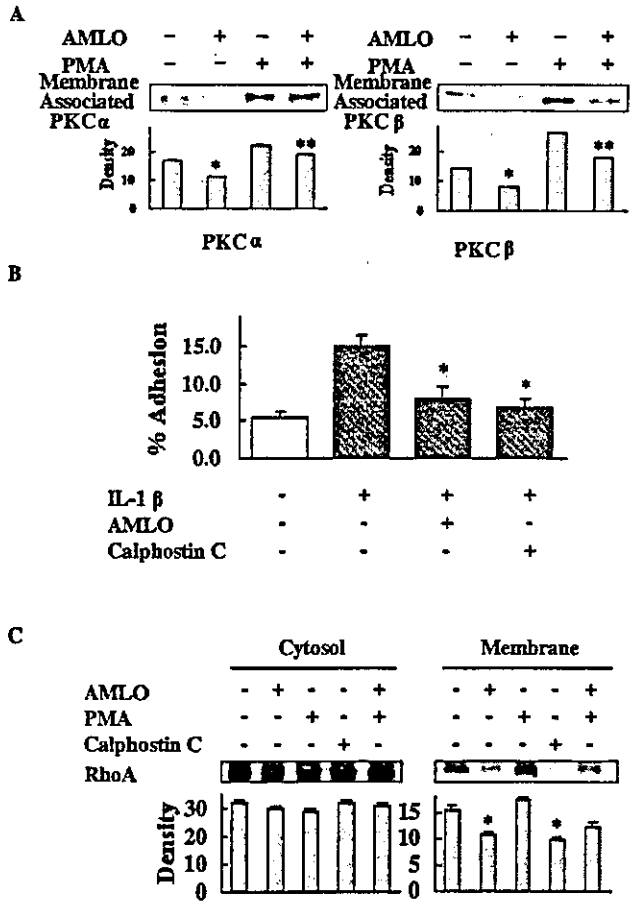


Figure 3. A, Effects of amlodipine on PKC activation in THP-1 cells. THP-1 cells ($10^6$/mL) were incubated in the presence of 10 μmol/L amlodipine [AMLO(+)] or medium alone [AMLO(−)] for 48 hours or pretreated with 100 ng/mL PMA for 10 minutes. Western blotting (10 μg protein/lane) detected PKC expression in membrane and cytosol lysates of THP-1 cells ($10^6$/mL) for each condition. Band densities were quantified by using an LAS1000 (FujiFilm) and are expressed in the bar graph shown. Blots are representative of 5 separate experiments. *$P$<0.001 vs AMLO(−), PMA(-). **$P$<0.001 vs AMLO(−), PMA(−). B, Inhibition of PKC attenuates THP-1 adhesion to activated HUVECs. THP-1 cells ($2\times10^6$/mL) were incubated with 10 μmol/L amlodipine [AMLO(+)] for 48 hours or 2 μmol/L calphostin C, and static adhesion assays were carried out in HUVEC monolayers activated with 10 U/mL IL-1β for 4 hours [IL-1β(+)]. Data are representative of 5 separate experiments. *$P$<0.005 vs IL-1β(+), AMLO(−), calphostin C(−). C, Inhibition of PKC inactivates RhoA in THP-1 cells. THP-1 cells ($10^6$/mL) were incubated in the presence of 10 μmol/L amlodipine [AMLO(+)] or medium alone [AMLO(−)] for 48 hours after pretreatment with 100 ng/mL PMA for 10 minutes or 500 nmol/L calphostin C for 30 minutes. Western blotting (10 μg protein/lane) detected RhoA expression in membrane and cytosol lysates of THP-1 cells ($10^6$/mL) for each condition. Band densities were quantified by using an LAS1000 (FujiFilm) and are expressed in the bar graph shown. Blots are representative of 5 separate experiments. *$P$<0.005 vs AMLO(−), PMA(−), calphostin C(−).

## Intracellular Concentration of Calcium Is Modulated by Amlodipine in THP-1 Cells

To investigate the effect of amlodipine on $[Ca^{2+}]_i$ in THP-1 cells, $[Ca^{2+}]_i$ was measured in THP-1 cells after stimulation with PMA. When THP-1 cells were preincubated with amlodipine, the increase in $[Ca^{2+}]_i$ in response to PMA was dramatically diminished (Figure 4A). Furthermore, when

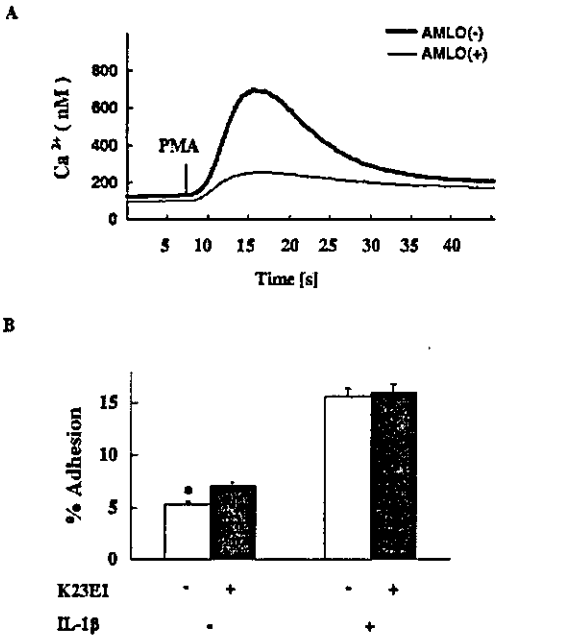


Figure 4. A, Effect of amlodipine on $[Ca^{2+}]_i$ in THP-1 cells. THP-1 cells ($10^6$ cells) were preincubated in the presence [AMLO(+)] or absence [AMLO(−)] of amlodipine for 48 hours and then resuspended in DPBS buffer. $[Ca^{2+}]_i$ was measured after addition of PMA (10 ng/mL) as described in Methods. Data represent the mean of 6 different experiments. The SD was within 5%. B, Effect of calcium ionophore K23E1 on THP-1 cell adhesion to vascular endothelium. THP-1 cells ($2\times10^6$ cells) were stimulated with calcium ionophore K23E1 (1 μmol/L) for 15 seconds before adhesion assay. HUVEC monolayers in a 96-well plate were stimulated with IL-1β, and an adhesion assay was performed as described in Methods. Data represent the mean of 6 different experiments. *$P$<0.005 vs K23E1(+), IL-1β(−).

THP-1 cells were pretreated with the calcium ionophore K23E1 to increase the level of $[Ca^{2+}]_i$, the adhesion of THP-1 cells to activated HUVECs was increased (Figure 4B).

## Amlodipine Reduces Activated $\beta_1$-Integrin in THP-1 Cells

To investigate the involvement of integrin activation, Western blotting analysis was performed with the monoclonal antibody HUTS21 to detect an activation-dependent epitope of $\beta_1$-integrin in THP-1 cells. HUTS21-positive $\beta_1$-integrin was significantly increased after incubation with amlodipine in THP-1cells, whereas immunoreactivity against 4B7R, a monoclonal antibody that detects constitutively expressed epitopes of $\beta_1$-integrin, was not changed (Figure 5).

## Discussion

We investigated the effects of amlodipine on the adhesion of monocytes to vascular endothelium under flow conditions. Incubation of monocytic THP-1 cells with amlodipine significantly inhibited their adhesion to HUVECs in the presence of flow. Recent study results have indicated that certain calcium channel blockers might possess an ability to prevent atherosclerosis in vivo,[10–12] and several in vitro findings have shown an inhibition of smooth muscle cell proliferation[13,14] and cytokine production[15,16] by amlodipine. Moreover, a

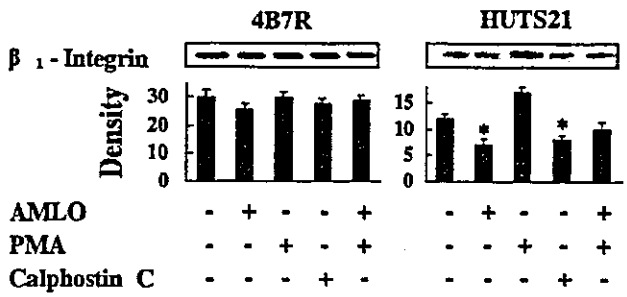


**Figure 5.** Activation of $\beta_1$-integrin was reduced after amlodipine treatment. THP-1 cells were treated as described in the legend to Figure 3C. Activation-dependent epitopes of $\beta_1$-integrin (HUTS21) and total $\beta_1$-integrin (4B7R) expression were detected for each condition by Western blotting analysis (10 $\mu$g protein/lane). Blots are representative of 5 separate experiments. Bar graph shows the ratios of activation-dependent epitope expression to total $\beta_1$-integrin expression from 5 separate experiments. *$P$<0.005 vs AMLO(−), PMA(−), calphostin C(−).

recent prospective study of amlodipine that used a randomized evaluation method clearly suggested its dramatic efficacy in reducing cardiac events.[17] However, the mechanism by which this calcium channel blocker modulates atherosclerosis is not yet fully understood, although recent results have indicated a reduction of plasma soluble vascular cell adhesion molecule-1 after treatment with amlodipine for 3 weeks,[18] suggesting an anti-inflammatory role for this compound.

Thus far, nonexcitable cells, including monocytes and lymphocytes, have been shown to possess a store-operated calcium channel (SOC), however, not a voltage-operative calcium channel (VOC) or an L-type $Ca^{2+}$ channel. As a result, dihydropyridines, which are potent antagonists of the L-type $Ca^{2+}$ channel, are not considered to be effective with these cell types. On the other hand, a recently identified SOC has been proposed as a mammalian homologue of the transient receptor potential gene product of *Drosophila* photoreceptors, which shares a strong homology with VOC.[19,20] These structural similarities indicate that specific compounds that target the VOC might also function against the SOC. In fact, in the present study, we demonstrated that amlodipine was able to reduce the PMA-induced calcium influx in THP-1 cells, which might potentially explain the antiatherosclerotic effect of this compound, although the precise mechanism of this effect remains to be elucidated.

Our present observations of the inhibitory effects of amlodipine toward THP-1 adhesion to vascular endothelium might be important evidence in support of the antiatherosclerotic potential of this compound, because, as has already been shown, the adhesion of monocytes to vascular endothelium is believed to be one of the crucial steps of atherogenesis. However, it is important to note that cell surface expression of adhesion receptors was not changed by amlodipine treatment. Although the dynamic interaction between leukocytes and endothelial cells is mainly regulated by physical binding of adhesion molecules on both sides,[21] the intracellular environment, such as the cytoskeleton and related signal-transduction cascades, has also been shown to play an equally important role in this mechanism.[7,22] Therefore, we investigated the effects of amlodipine on the relevant intracellular mechanism(s) of THP-1 cells that might modulate monocyte-endothelial interactions.

We also examined the potential participation of RhoA GTPase in amlodipine-induced antiadhesive effects in THP-1 cells, because RhoA GTPase has been shown to be one of the critical regulators of cell motility and cytoskeleton functions.[6,23] We previously documented the importance of RhoA GTPase in the regulation of monocyte adhesion to vascular endothelium by using monocytes pretreated with a 3-hydroxy-3-methylglutaryl coenzyme A reductase inhibitor, or statin.[6] In the present study, we demonstrated for the first time that amlodipine, a dihydropyridine, was able to modulate the activation of RhoA GTPase in monocytic cells. Although a similar inhibitory action toward RhoA has been shown with statin, the responsible mechanism underlying the observed effects of amlodipine are quite distinct, as dihydropyridines are not likely to inhibit intracellular cholesterol synthesis or the several important intermediates required for activation of small GTP proteins, including RhoA GTPase.[24,25] Recent studies with intestinal epithelial cells have also suggested that the $[Ca^{2+}]_i$ has an effect of the regulation of RhoA activation.[26] Therefore, as we showed, manipulation of the $[Ca^{2+}]_i$ was able to modulate cell migration via RhoA activation.

Knowledge of the participation of PKC-$\alpha$ and -$\beta$ upstream of RhoA GTPase has further advanced our understanding of these effects, and recent observations suggest that PKC is the molecular target of ischemia-induced endothelial cell permeability, which is protected by dihydropyridines.[27] We observed an effect of amlodipine on PKC isoforms $\alpha$ and $\beta$, but not $\delta$ or $\iota$. The importance of PKC-$\alpha$ and -$\beta$ during cell adhesion has been previously reported,[27,28] as Sun et al[28] showed that overexpression of PKC-$\alpha$ enhanced the motility and adhesion of breast cancer cells and Nonaka et al[29] found that inhibition of PKC-$\beta$ resulted in reduced entrapment of leukocytes in rat diabetic retina models. Using a specific inhibitor of PKC, we were able to document a critical role for PKC in monocyte-endothelial interactions in the present study.

It is of great interest to elucidate how amlodipine modulates the activation of PKC in THP-1 cells. One possible explanation is that amlodipine interferes with the release of phospholipid components, such as diacylglycerol, from the plasma membrane to activate PKC.[27] As previously reported, disturbance of this phospholipid would dramatically affect PKC signaling.[30] Furthermore, the unique characteristics of amlodipine that cause it to exhibit a strong and sustained affinity to the lipid bilayer might play a role in the amlodipine-dependent reduction of THP-1 cell adhesion.

## Perspectives

We found that treatment with amlodipine, a calcium channel antagonist, significantly inhibited monocytic THP-1 cell adhesion to cytokine-activated vascular endothelium under flow conditions. The potential mechanisms seemed to involve inhibition of PKC ($\alpha$ and $\beta$), RhoA GTPase, and the actin cytoskeleton by reducing $[Ca^{2+}]_i$. Although we did not examine other compounds of this class, the lipophilic property of amlodipine might be important to exert this effect. Our results

indicate a novel antiatherosclerotic role for this compound, though at relatively high concentrations, which might be independent of its effect on L-type calcium channels.

## Acknowledgments

The authors gratefully acknowledge support (10178102) and special coordination funds from the Ministry of Education, Science, Technology and Culture of Japan. We also wish to thank Dr Mitsuhiko Koresawa of the Department of Obstetrics, Sanraku Hospital, Tokyo, for supplying the umbilical cords, along with Yoshie Nakamura and Megumi Hiraoka for their technical assistance.

## References

1. Nayler WG. The antiatherogenic effects of amlodipine: promise of preclinical data. *J Hum Hypertens.* 1992;6:S19–S23.
2. Hoshida S, Yamashita N, Kuzuy T, Hori M. Reduction in infarct size by chronic amlodipine treatment in cholesterol-fed rabbits. *Atherosclerosis.* 1998;138:163–170.
3. Sima A, Stancu C, Constantinescu E, Ologeanu L, Simionescu M. The hyperlipemic hamster: a model for testing the anti-atherogenic effect of amlodipine. *J Cell Mol Med.* 2001;5:153–162.
4. Zhang XP, Hintze TH. Amlodipine releases nitric oxide from canine coronary microvessels. *Circulation.* 1998;97:576–580.
5. Ishii H, Yoshida M, Rosenzweig A, Gimbrone MA Jr, Yasukochi Y, Numano F. Adenoviral transduction of human E-selectin into isolated, perfused, rat aortic segments: an ex vivo model for studying leukocyte-endothelial interactions. *J Leukoc Biol.* 2000;68:687–692.
6. Yoshida M, Sawada T, Ishii H, Gerszten RE, Rosenzweig A, Gimbrone M Jr, Yasukochi Y, Numano F. HMG-CoA reductase inhibitor modulates monocyte–endothelial cell interaction under physiological flow conditions in vitro involvement of Rho GTPase-dependent mechanism. *Arterioscler Thromb Vasc Biol.* 2001;21:1165–1171.
7. Wojciak-Stothard B, Williams L, Ridley AJ. Monocyte adhesion and spreading on human endothelial cells is dependent on Rho-regulated receptor clustering. *J Cell Biol.* 1999;145:1293–1307.
8. Mochly-Rosen D, Gordon AS. Anchoring proteins for protein kinase C: a means for isozyme selectivity. *FASEB J.* 1998;12:35–42.
9. Mamputu JC, Renier G. Differentiation of human monocytes to monocyte-derived macrophages is associated with increased lipoprotein lipase-induced tumor necrosis factor-$\alpha$ expression and production: a process involving cell surface proteoglycans and protein kinase C. *Arterioscler Thromb Vasc Biol.* 1999;19:1405–1411.
10. Schmitz G, Hankowitz J, Kovacs EM. Cellular processes in atherogenesis: potential targets of $Ca^{2+}$ channel blockers. *Atherosclerosis.* 1991; 88:109–132.
11. Tulenko TN, Laury-Kleintop L, Walter MF, Mason RP. Cholesterol, calcium and atherosclerosis: is there a role for calcium channel blockers in atheroprotection? *Int J Cardiol.* 1997;62:S55–S66.
12. Chen L, Haught WH, Yang B, Saldeen TG, Parathasarathy S, Mehta JL. Preservation of endogenous antioxidant activity and inhibition of lipid peroxidation as common mechanisms of antiatherosclerotic effects of vitamin E, lovastatin and amlodipine. *J Am Coll Cardiol.* 1997;30: 569–575.
13. Stepien O, Gogusev J, Zhu DL, Iouzalen L, Herembert T, Drueke TB, Marche P. Amlodipine inhibition of serum-, thrombin-, or fibroblast growth factor-induced vascular smooth-muscle cell proliferation. *J Cardiovasc Pharmacol.* 1998;31:786–793.
14. Lai YM, Fukuda N, Su JZ, Suzuki R, Ikeda Y, Takagi H, Tahira Y, Kanmatsuse K. Novel mechanisms of the antiproliferative effects of amlodipine in vascular smooth muscle cells from spontaneously hypertensive rats. *Hypertens Res.* 2002;25:109–115.
15. Rodler S, Roth M, Nauck M, Tamm M, Block LH. $Ca^{2+}$-channel blockers modulate the expression of interleukin-6 and interleukin-8 genes in human vascular smooth muscle cells. *J Mol Cell Cardiol.* 1995;27: 2295–2302.
16. Matsumori A, Ono K, Nishio R, Nose Y, Sasayama S. Amlodipine inhibits the production of cytokines induced by ouabain. *Cytokine.* 2000; 12:294–297.
17. Pitt B, Byington RP, Furberg CD, Hunninghake DB, Mancini GB, Miller ME, Riley W. Effect of amlodipine on the progression of atherosclerosis and the occurrence of clinical events: PREVENT Investigators. *Circulation.* 2000;102:1503–1510.
18. Turchetti V, Bellini MA, Boschi L, Postorino G, Pallassini A, Richichi MG, Trabalzini L, Guerrini M, Forconi S. Haemorheological and endothelial-dependent alterations in heart failure after ACE inhibitor, calcium antagonist and $\beta$ blocker. *Clin Hemorheol Microcirc.* 2002;27:209–218.
19. Phillips AM, Bull A, Kelly LE. Identification of a *Drosophila* gene encoding a calmodulin-binding protein with homology to the *trp* phototransduction gene. *Neuron.* 1992;8:631–642.
20. Willmott NJ, Choudhury Q, Flower RJ. Functional importance of the dihydropyridine-sensitive, yet voltage-insensitive store-operated $Ca^{2+}$ influx of U937 cells. *FEBS Lett.* 1996;394:159–164.
21. Butcher EC. Leukocyte-endothelial cell recognition: three (or more) steps to specificity and diversity. *Cell.* 1991;67:1033–1036.
22. Yoshida M, Westlin WF, Wang N, Ingber DE, Rosenzweig A, Resnick N, Gimbrone M Jr. Leukocyte adhesion to vascular endothelium induces E-selectin linkage to the actin cytoskeleton. *J Cell Biol.* 1996;133: 445–455.
23. Liu L, Moesner P, Kovach NL, Bailey R, Hamilton AD, Sebti SM, Harlan JM. Integrin-dependent leukocyte adhesion involves geranylgeranylated protein(s). *J Biol Chem.* 1999;274:33334–33340.
24. Goldstein JL, Brown MS. Regulation of the mevalonate pathway. *Nature.* 1990;343:425–430.
25. Fenton RG, Kung HF, Longo DL, Smith MR. Regulation of intracellular actin polymerization by prenylated cellular proteins. *J Cell Biol.* 1992; 117:347–356.
26. Rao JN, Li L, Golovina VA, Platoshyn O, Strauch ED, Yuan JX, Wang JY. $Ca^{2+}$-RhoA signaling pathway required for polyamine-dependent intestinal epithelial cell migration. *Am J Physiol Cell Physiol.* 2001;280: C993–C1007.
27. Hempel A, Lindschau C, Maasch C, Mahn M, Bychkov R, Noll T, Luft FC, Haller H. Calcium antagonists ameliorate ischemia-induced endothelial cell permeability by inhibiting protein kinase C. *Circulation.* 1999; 99:2523–2529.
28. Sun XG, Rotenberg SA. Overexpression of protein kinase C-$\alpha$ in MCF-10A human breast cells engenders dramatic alterations in morphology, proliferation, and motility. *Cell Growth Diff.* 1999;10:343–352.
29. Nonaka A, Kiryu J, Tsujikawa A, Yamashiro K, Miyamoto K, Nishiwaki H, Honda Y, Ogura Y. PKC-$\beta$ inhibitor (LY333531) attenuates leukocyte entrapment in retinal microcirculation of diabetic rats. *Invest Ophthalmol Vis Sci.* 2000;41:2702–2706.
30. Nishizuka Y. Intracellular signaling by hydrolysis of phospholipids and activation of protein kinase C. *Science.* 1992;258:607–614.

Available online at www.sciencedirect.com
SCIENCE DIRECT®
Biochemical and Biophysical Research Communications 310 (2003) 1062–1066
BBRC
www.elsevier.com/locate/ybbrc

# Introduction of short interfering RNA to silence endogenous E-selectin in vascular endothelium leads to successful inhibition of leukocyte adhesion

Yasunobu Nishiwaki,[a,c,1] Takanori Yokota,[b,1] Megumi Hiraoka,[a] Makoto Miyagishi,[d] Kazunari Taira,[d] Mitsuaki Isobe,[c] Hidehiro Mizusawa,[b] and Masayuki Yoshida[a,*]

[a] *Department of Medical Biochemistry, Tokyo Medical and Dental University Tokyo, Japan*
[b] *Department of Neurology and Neurological Science, Tokyo Medical and Dental University Tokyo, Japan*
[c] *Department of Cardiology, Tokyo Medical and Dental University Tokyo, Japan*
[d] *Department of Chemistry and Biotechnology, School of Engineering, The University of Tokyo, Japan*

Received 28 August 2003

**Abstract**

Short interfering RNAs (siRNAs) are powerful sequence-specific reagents that suppress gene expression in mammalian cells. We report for the first time that gene silencing of endothelial E-selectin by siRNAs leads to successful inhibition of leukocyte–endothelial interaction under flow. siRNAs designed to target human E-selectin were tranfected into human umbilical vein endothelial cells (HUVEC). Western blotting analysis revealed that transfection of these siRNAs, but not the scrambled control siRNA (100 nM each), attenuated E-selectin expression in HUVEC activated with TNF-α (10 ng/ml, 4 h) without affecting expression of ICAM-1. Moreover, a leukocyte adhesion assay under flow (shear stress = 1.0 dyne/cm$^2$) demonstrated that HUVEC transfected with a siRNA against E-selectin (siE-01) supported significantly less HL60 adhesion as compared to those transfected with the control siRNA (scE-01) after activation ($p < 0.03$). This technique provides a powerful strategy to dissect a specific function of a given molecule in leukocyte–endothelial interaction.


*Keywords:* Endothelial cells; Adhesion molecules; Molecular biology; Inflammation

Introduction of double-stranded RNAs (dsRNAs) has led to the development of a powerful sequence-specific tool to suppress gene expression during development in plants, invertebrates, and vertebrates [1]. In mammalian cell cultures, dsRNA-mediated interference of gene expression has also been accomplished by transfection of synthetic RNA oligonucleotides [2] or plasmids [3], with the requirement that the active fragments to be composed of 21 or 22 base pairs (short interfering RNA, siRNA) to ensure their specificity [4]. Application of siRNAs to abrogate endogenous gene expression in mammalian tissues is now regarded as a potentially powerful technique to define the function of a given molecule, as well as a possible method for gene therapy [5]. In the present study, we demonstrated that oligonucleotide-mediated delivery of siRNAs into vascular endothelium specifically reduced endogenous expression of E-selectin upon cytokine stimulation and subsequently inhibited leukocyte adhesion to the endothelium under flow. Knowledge of the ability of siRNAs to silence a specific gene in vascular endothelium will extend their application to novel gene therapies in cardiovascular medicine.

## Materials and methods

*Molecular biology procedures.* siRNAs were designed to target the coding sequence of human E-selectin cDNA. The target sequences were directed to the single-strand region according to the predicted secondary RNA structure and sequences of the form $(AA/CA)N_{19}$ with

* Corresponding author. Fax: +81-3-5800-3380.
*E-mail address:* masavasc@tmd.ac.jp (M. Yoshida).
[1] These two autohors equally contributed to the work.

0006-291X/$ - see front matter © 2003 Elsevier Inc. All rights reserved.
doi:10.1016/j.bbrc.2003.09.125

GC contents of less than 70% were selected from this region [6]. Nineteen nucleotide RNAs followed by TT/TG were selected, then chemically synthesized, and gel-purified. For generation of double-stranded siRNAs, both strands were mixed, then heated to 95 °C for 2 min, and 70 °C for 1 min after which they were allowed to cool to room temperature. The final concentration of the siRNAs was 20 μM in 2 mM of magnesium chloride in 1 mM phosphate-buffered saline, pH 7.4. Sequences corresponding to the siRNAs were as follows: siRNA-01, nucleotide numbers 163–183 for the E-selectin coding region (GenBank Accesion No. NM000450); siRNA-02, 266–286; siRNA-03, 301–322; siRNA-04, 1243–1263; and siRNA-05, 1364–1384. Western blotting was performed using standard protocols with ECL reagents (Amersham-Pharmacia), with purified mouse antibodies against E-selectin (7A9 [7]) and ICAM-1 (BBIG-I1, Wako Chemical, Japan). Based on the results of the siRNA oligonucleotides, we constructed DNA-based vectors that expressed the sequence of siRNA-01 by our original method [3]. The vector expressed siRNA hairpins under control of the U6 promoter, which contained the 3′ end of the 21 nt sense-strand and the 5′ end of the 21 nt antisense-strand connected by a 21 nt loop sequence (UAGAAUUACAUCAAGGGAGAU). These sequences were inserted immediately downstream of the U6 promoter in a pUC19 (Takara).

*Cell culture and transfection.* HEK293 cells were cultured in DMEM supplemented with 10% FBS, 2 mM glutamine, 100 U/ml penicillin, and 100 mg/ml streptomycin (Invitrogen). Human umbilical vein endothelial cells (HUVEC) were established from umbilical cords as previously described [8]. Typically, cells were seeded at $5 \times 10^4$ in each C-6 well and then transfected the next day with 2 μl Lipofectin 2000 (Invitrogen) combined with 3 μl (HEK293 cells) or 5 μl (HUVEC) with 20 μM of the siRNA in 1 ml Optimem (final concentration of siRNA was 60 nM for HEK293 cells and 100 nM for HUVEC). In some experiments, 1 μg E-selectin cDNA (pAdRSV4-E-sel [7]) or a

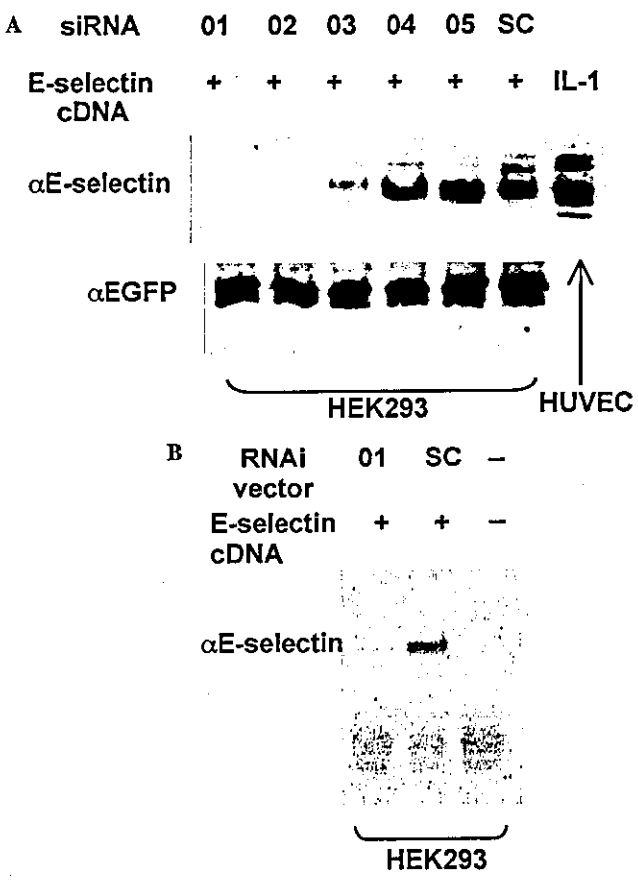


Fig. 1. (A) siRNA silencing of exogenous E-selectin gene expression in HEK293 cells. siRNA to human E-selectin (01 ~ 05) and a scrambled control siRNA 01 sequence (SC), each at 60 nM, were co-transfected into HEK293 cells with E-selectin cDNA (1 μg) and EGFP cDNA (1 μg) as described in Materials and methods. The cell lysates were subjected to Western blotting analysis using anti-E-selectin mAb (7A9). The lysate from HUVEC stimulated with IL-1β (IL-1) was used as positive control. Blots are representative of 4 similar experiments. (B) Efficacy of siRNA-vector against exogenous E-selectin gene expression in HEK293 cells. A U6 driven siRNA-vector to human E-selectin (01, 100 ng) and the control (SC, 100 ng) were co-transfected into HEK293 cells with E-selectin cDNA (1 μg) as described in Materials and methods. Western blotting analysis was carried out using an anti-E-selectin mAb (7A9). Blots are representative of 3 similar experiments.

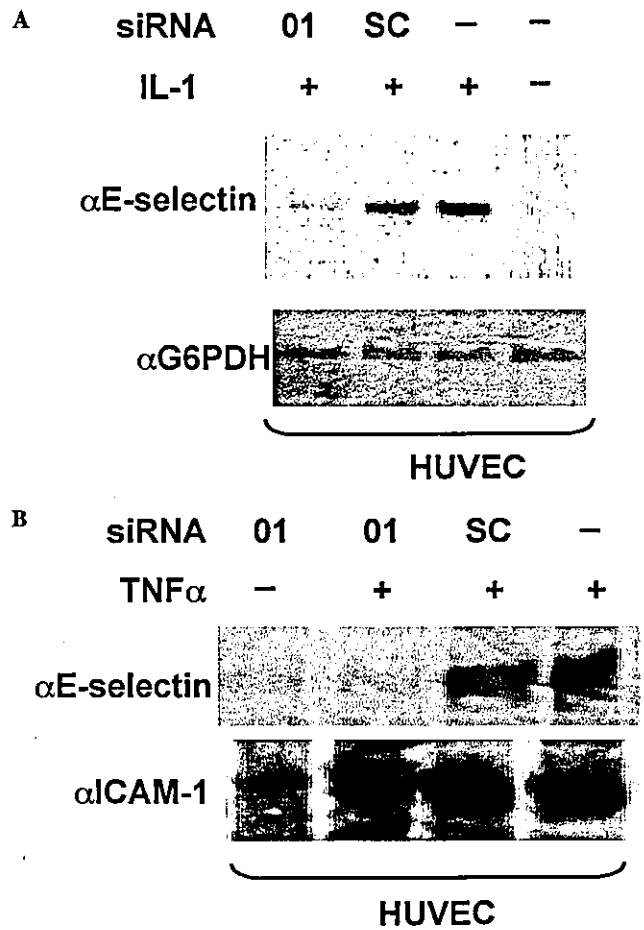


Fig. 2. (A) siRNA silencing of endogenous E-selectin gene expression in HUVEC. siRNA to human E-selectin (01) and a scrambled control of the siRNA 01 sequence (SC), each at 100 nM, were transfected into HUVEC as described in Materials and methods. Western blotting analysis was carried out using lysates prepared 24 h after transfection. The expression levels of G6PDH were also examined. Blots are representative of 3 similar experiments. (B) siRNA of E-selectin specifically inhibits gene expression of E-selectin but not ICAM-1 in activated HUVEC. siRNAs were transfected into HUVEC as described above, then 24 h after transfection, the HUVEC were stimulated with TNF-α (10 ng/ml) for 4 h, after which the cell lysates were prepared for Western blotting analysis to detect E-selectin and ICAM-1 expression.

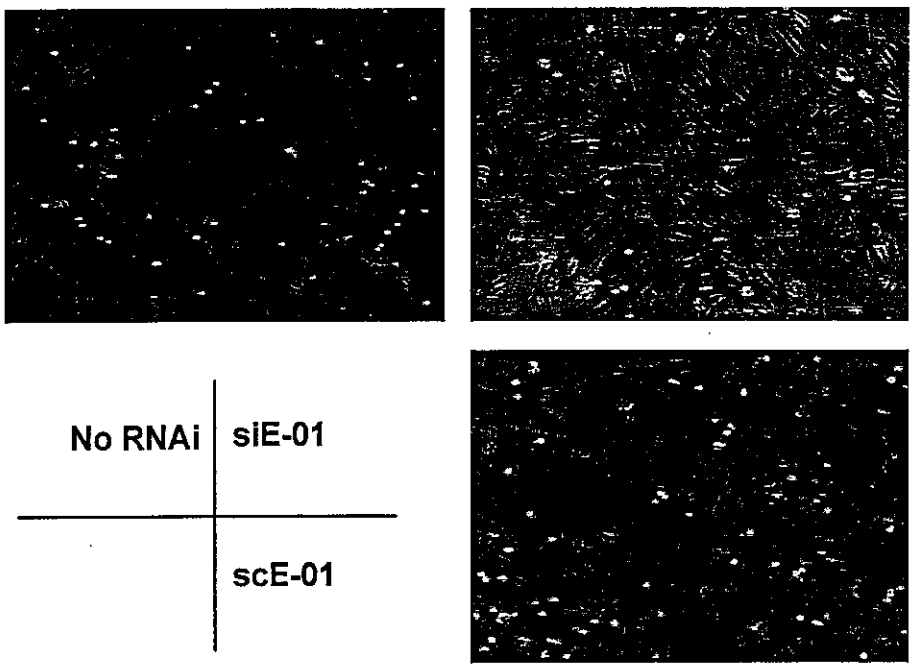


Fig. 3. siRNA of E-selectin specifically inhibits leukocyte adhesion to activated HUVEC under flow. siRNA to human E-selectin (siE-01) and a scrambled control of the siRNA 01 sequence (scE-01), each at 100 nM, were transfected into HUVEC and plated on a glass coverslip as described in Materials and methods. Twenty-four hours after transfection, the HUVEC were stimulated with TNF-α (10 ng/ml) for 4 h and an adhesion assay was carried out in the presence of laminar flow. Representative micrographs taken from video recording during the flow assay. HL-60 cells (white particles) were perfused over a TNF-activated HUVEC monolayer (gray background) that had been transfected with siE-01, scE-01, or lipofectin alone (no RNAi).

control plasmid containing enhanced green fluorescence protein (pEGFP-C2, Clontech) was co-transfected. Transfection mixtures were left on the cells for 16 h (HEK293 cells) or 4 h (HUVEC) and then replaced with regular media.

*In vitro flow assay.* The parallel-plate flow chamber used in the present study has been described previously in detail [9]. Briefly, HUVEC on coverslips were transfected with siRNA and then positioned in a flow chamber mounted on an inverted microscope. The monolayers were perfused for 5 min with perfusion medium [10] and HL60 cells ($10^5$ cells/ml) were then drawn through the chamber at controlled flow rate to generate a calculated wall shear stress of 1.0 dyne/cm$^2$ for 10 min. The entire period of perfusion was on videotape and then transferred to a PC for image analysis.

*Statistical analyses.* Results are presented as means ± SD. Data were analyzed using analysis of variance (ANOVA), with $p < 0.05$ considered significant.

## Results and discussion

First, we analyzed the efficacy of double-stranded, siRNAs to silence E-selectin gene expression using HEK293 cells co-transfected with human E-selectin cDNA. Five different siRNAs against the coding sequence of human E-selectin cDNA were designed and Western blotting analysis was carried out using cell lysates that had been prepared 24 h after transfection of the siRNAs. As shown in Fig. 1A, HEK293 cells transfected with 3 of the siRNAs (siE-01, siE-02, and siE-03) were able to inhibit co-transfected E-selectin expression; however, the other 2 (siE-04 and siE-05) as well as nucleic-acid-scrambled double-stranded RNA (scE-01) failed to inhibit E-selectin expression. Moreover, the specificity of gene silencing was confirmed using simultaneous transfection of pEGFP-C2 (Fig. 1A). Next we examined the efficacy of plasmid-mediated RNAi with E-selectin. RNAi-vectors were co-transfected with the E-selectin cDNA plasmid into HEK293 cells. As shown in Fig. 1B, Western blotting analysis 48 h after transfection clearly demonstrated that co-transfection of U6-siE-01 but not U6-control significantly reduced exogenous expression of E-selectin.

Based on these experiments, we decided to use siE-01 to suppress endogenous E-selectin expression in HUVEC. siE-01 and scE-01 (100 nM each) were transfected into HUVEC using a cationic-liposome-mediated method. To exclude the possibility of a non-specifc toxicity of the siRNAs, DAPI staining of HUVEC was carried out. The level of apoptotic HUVEC ratio was around 0.9%, suggesting that our RNAi transfection did not cause significant cell damage (data not shown). Twenty-four hours after siRNA transfection, HUVEC were activated with interleukin (IL) 1β (10 U/ml, 4 h). As shown in Fig. 2A, the IL-1β-induced E-selectin expression was significantly inhibited by siE-01 but not by scE-01. Further, the expression level of G6PDH was not changed by

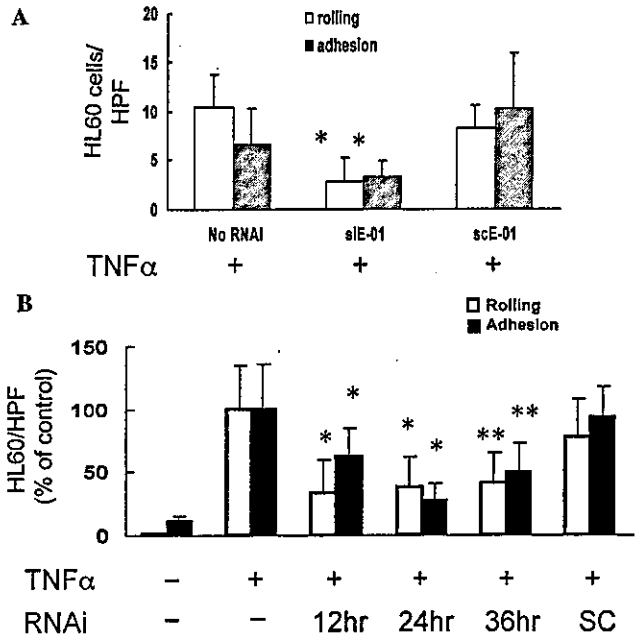


Fig. 4. Transfection of RNAi into HUVEC was performed as described in Fig. 3 and adhesion assay was carried out under flow (shear stress = 1.0 dyne/cm$^2$). (A) The number of adherent and rolling cells was quantitated from captured images using image analysis software and described as the number of interacting cells in each high power filled in the microscope area view (shear stress = 1.0 dyne/cm$^2$). *$p < 0.05$ vs. NoRNAi. (B) A quantitative adhesion assay under flow was carried out using HUVEC treated with siE-01 for various incubation times and compared to those treated with control RNA (SC) for 24 h (shear stress = 1.0 dyne/cm$^2$). *$p < 0.0005$ vs. TNF (+) RNAi (−), **$p < 0.005$ vs. TNF (+) RNAi (−). Data are representative of 4 similar experiments.

siRNA transfection. To validate the specificity of the inhibitory effects of siRNA, the expression level of ICAM-1 was also examined, however, it was not significantly altered after transfection of siE-01 (Fig. 2B). These results strongly suggested that introduction of siE-01 specifically silenced the expression of E-selectin.

Finally, leukocyte adhesion assay under flow was carried out using HUVEC transduced with siRNAs. As shown in Figs. 3 and 4A, the TNF-α-activated HUVEC monolayer supported a significantly greater adhesion of HL-60 cells under flow (shear stress = 1.0 dyne/cm$^2$) as compared to the non-activated HUVEC monolayer. Notably, the siE-01-transduced HUVEC monolayer failed to exhibit a comparable adhesion of HL-60 cells, whereas no inhibition of HL-60 adhesion was observed with the HUVEC monolayer transduced with sCE-01. We were able to inhibit E-selectin expression in activated HUVEC for up to 36 h after siE-01 transfection (Fig. 4B).

Our results may lead to the establishment of a novel experimental system to critically access the function of E-selectin in vascular endothelium using siRNA-mediated post transcriptional gene silencing. This is the first observation in the field of cardiovascular research of this novel technique, indeed, enabling us to manipulate a gene expressed in the vasculature. For the first time, we demonstrated that the lack of E-selectin gene expression significantly disrupted leukocyte–endothelial interaction in vascular endothelium and also showed that DNA-based siRNA expression vectors are effective against E-selectin in HEK293 cells. When considering applications for this siRNA approach to a potential gene therapy [11], an oligonucleotide-based system is advantageous in regard to biosafety. However, with gene therapy for atherosclerosis in vivo, a method to achieve long-term expression of siRNA in endothelium must be developed. For this purpose, we engineered similarly effective DNA-vector-based expressing siRNA, which might allow for long-term gene suppression in vivo with virus vectors, such as adeno-associate virus or renti-virus.

In conclusion, the efficacy of siRNA and our siRNA-expressing vector model to inhibit E-selectin-dependent leukocyte adhesion suggests that this RNA-targeting approach may provide a novel therapeutic option for inflammation and atherosclerotic disorders.

## Acknowledgments

This study was supported in part by grants from the Ministry of Education, Science, Sports and Culture of Japan, and from Ministry of Health, Labour and Welfare of Japan. We gratefully acknowledge the expert assistance of Noriko Nitta in working with the cell cultures.

## References

[1] G.J. Hannon, RNA interference, Nature 418 (2002) 244.
[2] S.M. Elbashir, W. Lendeckel, T. Tuschl, RNA interference is mediated by 21- and 22-nucleotide RNAs, Genes Dev. 15 (2001) 188.
[3] M. Miyagishi, K. Taira, U6 promoter-driven siRNAs with four uridine 3′ overhangs efficiently suppress targeted gene expression in mammalian cells, Nat. Biotechnol. 20 (2002) 497.
[4] L. Manche, S.R. Green, C. Schmedt, M.B. Mathews, Interactions between double-stranded RNA regulators and the protein kinase DAI, Mol. Cell. Biol. 12 (1992) 5238.
[5] D.P. Cioca, Y. Aoki, K. Kiyosawa, RNA interference is a functional pathway with therapeutic potential in human myeloid leukemia cell lines, Cancer Gene Ther. 10 (2003) 125.
[6] S.M. Elbashir, J. Harborth, W. Lendeckel, A. Yalcin, K. Weber, T. Tuschl, Duplexes of 21-nucleotide RNAs mediate RNA interference in cultured mammalian cells, Nature 411 (2001) 494.
[7] M. Yoshida, B.E. Szente, J.M. Kiely, A. Rosenzweig, M.A. Gimbrone Jr., Phosphorylation of the cytoplasmic domain of E-selectin is regulated during leukocyte-endothelial adhesion, J. Immunol. 161 (1998) 933.
[8] M. Yoshida, W.F. Westlin, N. Wang, D.E. Ingber, A. Rosenzweig, N. Resnick, M.A. Gimbrone Jr., Leukocyte adhesion to vascular endothelium induces E-selectin linkage to the actin cytoskeleton, J. Cell Biol. 133 (1996) 445.
[9] A. Kawakami, A. Tanaka, K. Nakajima, K. Shimokado, M. Yoshida, Atorvastatin attenuates remnant lipoprotein-induced

monocyte adhesion to vascular endothelium under flow conditions, Circ. Res. 91 (2002) 263.
[10] M. Yoshida, T. Sawada, H. Ishii, R.E. Gerszten, A. Rosenzweig, M.A. Gimbrone Jr., Y. Yasukochi, F. Numano, HMG-CoA reductase inhibitor modulates monocyte–endothelial cell interaction under physiological flow conditions in vitro: involvement of RhoA GTPase-dependent mechanism, Arterioscler. Thromb. Vasc. Biol. 21 (2001) 1165.
[11] J.M. Jacque, K. Triques, M. Stevenson, Modulation of HIV-1 replication by RNA interference, Nature 418 (2002) 435.

# Pioglitazone reduces monocyte adhesion to vascular endothelium under flow by modulating RhoA GTPase and focal adhesion kinase

Yasutoshi Toriumi[a,b], Megumi Hiraoka[a], Mamoru Watanabe[b], Masayuki Yoshida[a,*]

[a] *Department of Vascular Medicine, Medical Biochemistry, Tokyo Medical and Dental University, 1-5-45, Yushima Bldg. D-256, Bunkyo-ku, Tokyo 113-8519, Japan*

[b] *Department of Gastroenterology and Hepatology, Tokyo Medical and Dental University, Tokyo, Japan*

Received 1 July 2003; revised 25 August 2003; accepted 8 September 2003

First published online 3 October 2003

Edited by Beat Imhof

**Abstract Thiazolidinediones (TZDs), potent peroxisome proliferator-activated receptor γ ligands, have been shown to improve endothelial function in vascular diseases. We investigated the effects of pioglitazone, a TZD, on monocyte–endothelial interaction under flow and found that pretreatment (20 μmol/l, 48 h) significantly reduced U937 adhesion to human umbilical vein endothelial cells. Integrin expression was not altered, however, the activation of RhoA GTPase was significantly reduced after treatment. Further, pioglitazone treatment significantly reduced phosphorylation of focal adhesion kinase (FAK) at 925Y, but not at 397Y, suggesting a specific role in FAK-dependent signaling. These results indicate a novel anti-inflammatory role for this compound.**



*Key words:* Thiazolidinedione; Monocyte adhesion; Cytoskeletal organization; Atherosclerosis

## 1. Introduction

Thiazolidinediones (TZDs) are insulin-sensitizing compounds that have been used to treat patients with type 2 diabetes. TZD compounds have been identified as a ligand for peroxisome proliferator-activated receptor γ (PPARγ), which belongs to a nuclear hormone receptor superfamily, and also received attention for their potential anti-inflammatory effects. Further, PPARγ activators such as 15-deoxy-12,14-prostaglandin J2, and TZDs have been shown to inhibit the production of several inflammatory cytokines, including interleukin (IL) 1β, IL-6, and tumor necrosis factor α in monocytes [1], and inducible nitric oxide synthase, matrix metalloprotease-9, and scavenger receptor-A expression in macrophages [2], and have also been reported to have anti-inflammatory effects that are independent of PPARγ [3]. We investigated the inhibitory effects of pioglitazone, a TZD, on monocyte–endothelial interaction under flow conditions and examined the molecular consequences.

## 2. Materials and methods

### 2.1. Cell culture and reagents

A U937 cell line was obtained from the American Type Culture Collection (Rockville, MD, USA) and grown in RPMI 1640 medium supplemented with 10% fetal calf serum (Life Technologies Oriental, Tokyo, Japan). Human umbilical vein endothelial cells (HUVEC) were isolated from normal-term umbilical cords and maintained as previously described [4,5]. Recombinant human IL-1β was obtained from Genzyme (Cambridge, MA, USA). BCECF-AM and FITC-conjugated phalloidin were obtained from Molecular Probes (Eugene, OR, USA). Pioglitazone hydrochloride was a gift from Takeda Chemical Industry (Osaka, Japan) and was stored as a 20 mmol/l stock solution in dimethyl sulfoxide. Mouse anti-CD11a monoclonal antibody (clone 38, Ancell, Bayport, MN, USA); mouse anti-CD11b monoclonal antibody (clone 44, YLEM, Avezzano, Italy), mouse anti-CD18 monoclonal antibody (clone MEM48, Southern Biotechnology Associates, Birmingham, AL, USA), and mouse anti-CD49d monoclonal antibody (clone A4-PUJ1, Upstate Biotechnology, Lake Placid, NY, USA) were used in the present study. Rho activation assay kit was obtained from Upstate Biotechnology. Anti-focal adhesion kinase (FAK) monoclonal antibody was obtained from BD Biosciences (Franklin Lakes, NJ, USA). Anti-phosphorylated (p) FAK (397Y) monoclonal antibody and anti-pFAK (925Y) monoclonal antibody were obtained from Biosource (Camarillo, CA, USA). Horseradish peroxidase-conjugated goat anti-mouse IgG and anti-rabbit IgG were obtained from Cal-tag (Burlingame, CA, USA).

### 2.2. Monocyte adhesion assay

Static adhesion assays were carried out as previously described in detail [6]. In brief, U937 cells were prelabeled with BCECF-AM for 20 min at 37°C, and then placed on HUVEC plated in a 96-well microtiter culture plate and incubated for 10 min at room temperature. The fluorescent intensity of the monolayer-associated U937 cells was quantitated using a fluorescent plate reader (Perseptive Biosystems). Adhesion assays under laminar flow were carried out as described previously [7]. In brief, HUVEC monolayers on coverslips were stimulated with 10 U/m of IL-1β for 4 h, positioned in the flow chamber mounted on an inverted microscope (1×70, Olympus, Tokyo, Japan). U937 cells ($1\times10^6$/ml) were drawn through the chamber at a wall shear stress of 1.0 dyne/cm$^2$ for 10 min. The entire period of perfusion was recorded using a video tape recorder. The numbers of rolling and adherent U937 cells on HUVEC monolayer in 6–10 randomly selected 20× microscope fields were determined.

### 2.3. Filamentous actin content in U937 cells

U937 cells were washed twice with Dulbecco's Phosphate-Buffered Saline (DPBS) and fixed with 1% paraformaldehyde in DPBS for 5 min, then permeabilized with 0.1% Triton X-100 in DPBS for 60 s. U937 cells were then incubated with FITC-conjugated phalloidin (1:100 dilution) in DPBS for 60 min. After washing twice with DPBS, U937 cells were lysed with 150 μl of 0.01% NaOH in 0.1% sodium dodecyl sulfate (SDS) and fluorescent intensity was quantitated using a fluorescent plate reader.

### 2.4. RhoA translocation in U937 cells

RhoA translocation in U937 cells was examined by Western blotting analysis as described previously [8,9]. In brief, U937 cells were incubated with pioglitazone and then lysed in 100 μl of ice-cold lysis buffer (0.1 mol/l Tris–HCl, 0.15 mol/l NaCl, and 5 mmol/l EDTA, pH 7.4) containing 0.1% Triton X-100, 10 μg/ml leupeptin, 60 U/ml aprotinin, 1 mM phenylmethylsulfonyl fluoride, and 100 μmol/l sodium

*Corresponding author. Fax: (81)-3-5800 3380.
*E-mail address:* masavasc@tmd.ac.jp (M. Yoshida).

0014-5793/03/$22.00 
doi:10.1016/S0014-5793(03)01040-8

vanadate for 5 min, then centrifuged at 15000 rpm for 15 min. The supernatants were collected as the cytosol fractions of the cell lysate. Pellets were washed with phosphate-buffered saline and lysed for 5 min in 100 μl of ice-cold lysis buffer as described above, except that it contained 1% Triton X-100, after which they were centrifuged at 15000 rpm for 15 min. The supernatants were collected as the membrane fractions. To obtain a total cell lysate, U937 cells were lysed with 100 μl of ice-cold lysis buffer containing 1% Triton X-100 for 10 min. An equal amount of protein (10 μg) from each lysate was subjected to 12.5% SDS–polyacrylamide gel electrophoresis and Western blotting analysis was carried out using mouse anti-RhoA monoclonal antibody (1:500 dilution). Activation of RhoA was determined by using a glutathione *S*-transferase (GST) fusion protein of the Rho binding domain of the Rho effector Rhotekin (Rho activation assay kit) following the manufacturer's protocol.

*2.5. FAK phosphorylation in U937 cells*

Phosphorylation of FAK at both 925Y and 397Y in U937 cells was examined by Western blotting analysis using phosphorylation-specific monoclonal antibodies against FAK as described above.

*2.6. Statistical analysis*

Results are presented as mean ± S.D. Data were analyzed using analysis of variance. $P < 0.05$ was considered significant.

## 3. Results

*3.1. Pioglitazone reduced IL-1β-induced U937 cell adhesion to HUVEC*

We first examined the effect of pioglitazone on monocytic U937 adhesion to cytokine-activated HUVEC (IL-1β 10 U/ml, 4 h). U937 cells were pretreated with various concentrations (1, 5, 10 and 20 μmol/l) of pioglitazone for 48 h prior to an adhesion assay. As shown in Fig. 1A, a dose-dependent reduction of pioglitazone-treated U937 cell adhesion to HUVEC was observed at concentrations as low as 10 μmol/l of pioglitazone (control 21.8 ± 4.64% adhesion, 0.5 μmol/l 20.0 ± 2.89%, 10 μmol/l 8.45 ± 1.15% and 20 μmol/l 8.10 ± 1.82%). Since we did not detect significant cellular damage caused by these pioglitazone treatments using trypan blue staining (data not shown), we chose to treat the U937 cells with 20 μmol/l of pioglitazone in the following experiments. The inhibitory effects of pioglitazone on the adhesion of U937 cells to HUVEC were then examined under flow conditions at a laminar shear stress level of 1.0 dyne/cm$^2$. U937 cells were incubated in the presence of 20 μmol/l of pioglitazone for 48 h then perfused over HUVEC for 10 min. As shown in Fig. 1B, the adhesion, but not rolling, of U937 cells was significantly reduced after pioglitazone treatment (control 8.20 ± 3.03 cells/HPF (high power field); pioglitazone 2.40 ± 1.67 cells/HPF, $P < 0.006$).

*3.2. Effect of pioglitazone on integrin expression in U937 cells*

To elucidate the molecular mechanism of the pioglitazone-induced reduction of U937 cell adhesion, cell surface integrin expression after pioglitazone treatment was examined by flow cytometric analysis. The expression levels of CD11a, CD18, and CD49d on U937 cells were not significantly affected after treatment, as shown in Fig. 2A.

*3.3. Pioglitazone reduced actin polymerization and RhoA activation in U937 cells*

We then examined the effect of pioglitazone on the cytoskeletal network in U937 cells by detecting F-actin, which reflects actin polymerization. When U937 cells were incubated with 20 μmol/l of pioglitazone for 48 h, the F-actin content in

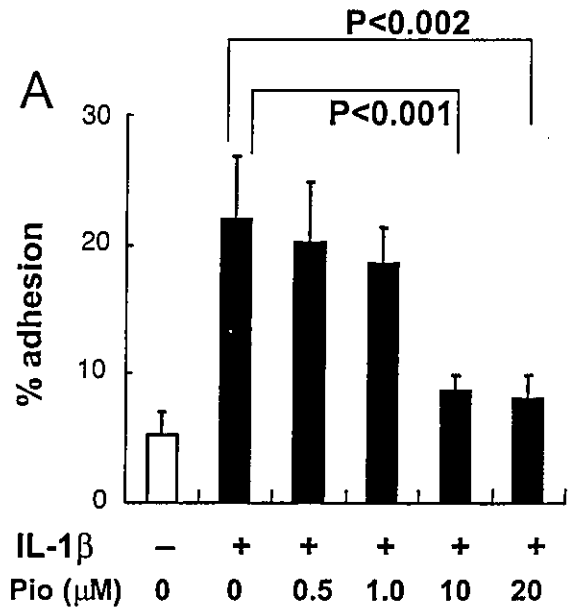


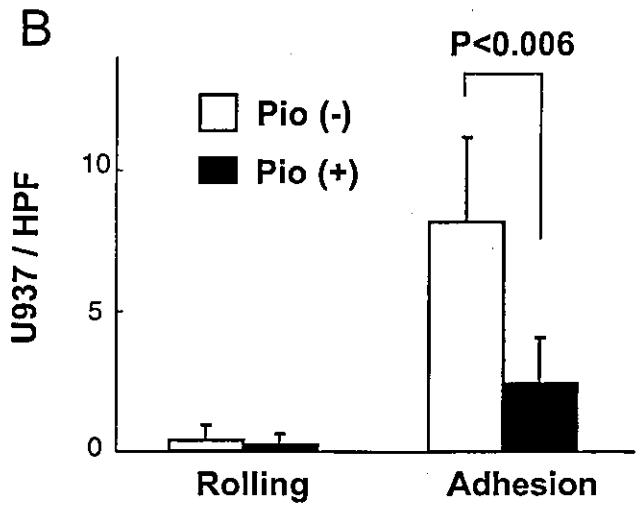


Fig. 1. Effect of pioglitazone on adhesion of U937 cells to HUVEC under static and physiological flow conditions. A: U937 cells ($1 \times 10^6$/ml) were incubated with the indicated amounts of pioglitazone for 48 h and then placed on HUVEC activated with 10 U/ml of IL-1β for 4 h. An adhesion assay was carried out as described in Section 2. B: U937 cells were treated with (+) or without (−) 20 μmol/l of pioglitazone for 48 h and then perfused over activated HUVEC monolayers at a flow rate of 1.0 dyne/cm$^2$. Rolling and adherent U937 cells on HUVEC were counted in 10 different 20× microscope fields as described in Section 2. Data are representative of three separate observations.

U937 cells was significantly decreased (0.64-fold of control, $P < 0.05$) (Fig. 2B). The effect of pioglitazone on RhoA GTPase activity in U937 cells was also examined by determining RhoA translocation from the cytoplasm to membrane and Rho pull-down assay using a GST fusion protein of the Rho effector Rhotekin. Western blotting analysis revealed that the expression of RhoA protein in the membrane fraction and Rhotekin-bound activated RhoA were significantly decreased in U937 cells after pioglitazone treatment (Fig. 2C).

### 3.4. Pioglitazone inhibited FAK activation in U937 cells

We also investigated the involvement of FAK in U937 cells. Western blotting analysis was carried out using antibodies to detect phosphorylation of FAK at two distinct tyrosines. As shown in Fig. 3A, the expression of total FAK was not affected by pioglitazone treatment, however, FAK phosphorylation at tyrosine 925 was significantly inhibited. In contrast, phosphorylation of FAK at tyrosine 397 was not affected by pioglitazone treatment.

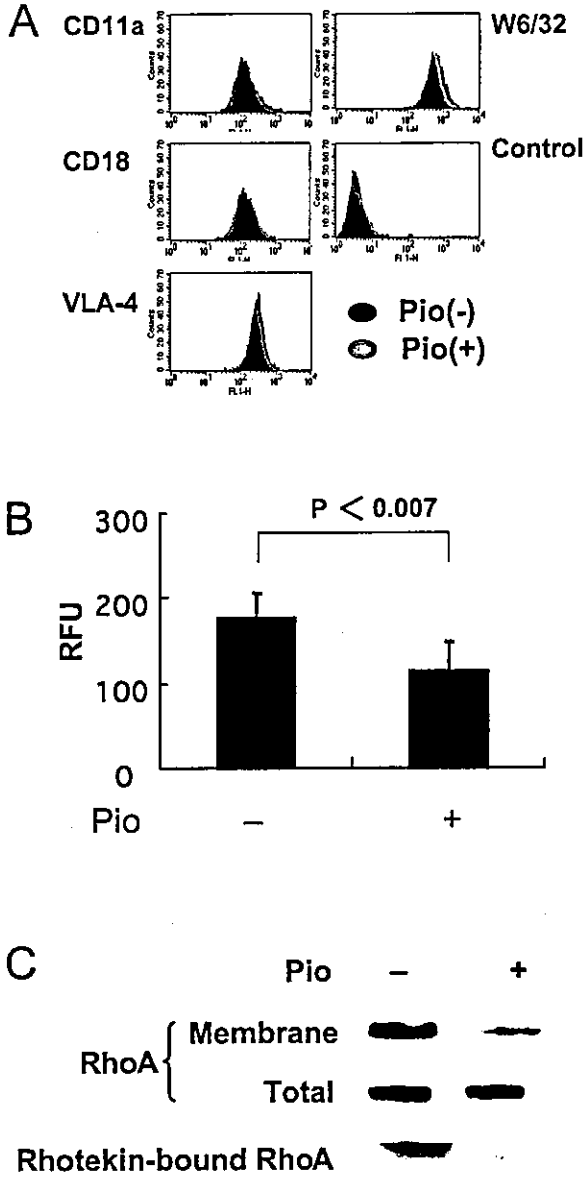


Fig. 2. Effect of pioglitazone on integrin expression, actin cytoskeleton, and RhoA GTPase in U937 cells. A: U937 cells ($1\times10^6$/ml) were incubated with 20 μmol/l of pioglitazone (+) or medium alone (−) for 48 h. Integrin expression in U937 cells was analyzed by flow cytometry analysis using monoclonal antibodies to integrins (CD11a, CD18, VLA4) and compared to positive control HLA class I (w6/32). Five thousand cells were analyzed for each condition. Data are representative of four similar experiments. B: U937 cells ($1\times10^6$/ml) were incubated with 20 μmol/l of pioglitazone or in medium alone (control) for 48 h. F-actin content in U937 cells was detected with phalloidin and quantitated using a fluorescent plate reader as described in Section 2, and then expressed as a percentage of that of the control. $^*P<0.05$ vs. control. Data are representative of three separate observations. C: U937 cells were incubated with medium alone (−) or 20 μmol/l of pioglitazone (+) for 48 h. Western blotting detected RhoA expression in the membrane and total lysate of U937 cells for each condition. RhoA activity was also determined using the Rhotekin assay. Blots are representative of three separate experiments.

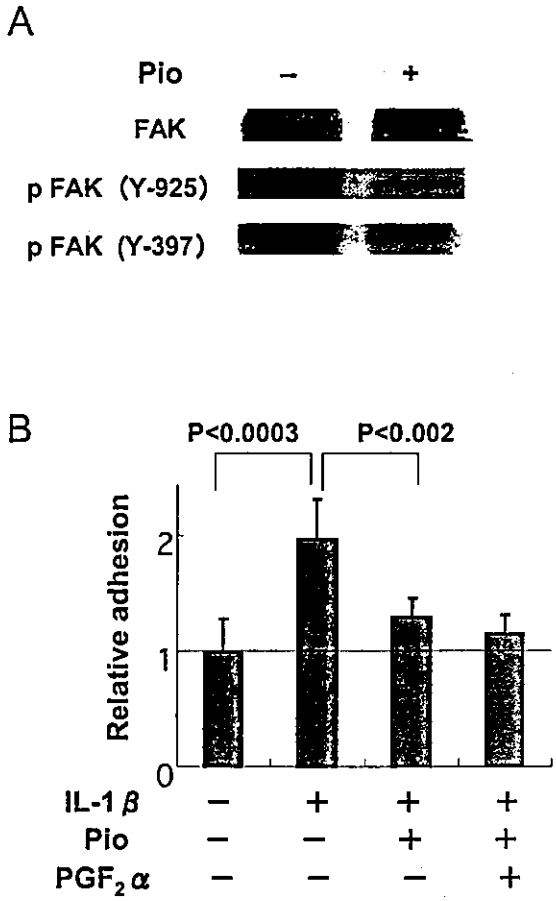


Fig. 3. A: Effects of pioglitazone on FAK activation in U937 cells. U937 cells ($1\times10^6$/ml) were incubated with 20 μmol/l of pioglitazone (+) or in medium alone (−) for 48 h. The expressions of pFAK (397Y), pFAK (925Y), and FAK were detected in each condition by Western blotting analysis. Blots are representative of five separate experiments. B: Effect of PPAR antagonist on adhesion of U937 cells to HUVEC. U937 cells ($1\times10^6$/ml) were incubated with 20 μmol/l of pioglitazone, PGF2α, for 30 min prior to incubation with 20 μmol/l of pioglitazone, or medium alone for 48 h, and then placed on HUVEC. An adhesion assay was carried out as described in Section 2.

### 3.5. PPAR antagonist failed to reverse the inhibitory effects of pioglitazone toward the adhesion of U937 cells to HUVEC

To examine whether the antagonizing PPARγ receptor has some effects on U937 adhesion, U937 cells were treated with prostaglandin F2α (PGF2α) for 30 min prior to pioglitazone treatment, in order to compete with the PPARγ binding of pioglitazone. When adhesion assays were carried out, pretreatment of U937 cells with PGF2α failed to reverse the inhibitory effects of pioglitazone toward the adhesion of U937 cells to the HUVEC monolayer (Fig. 3B).

## 4. Discussion

Recent studies have shown that TZDs have protective ef-

fects against atherosclerosis, as well as direct biological effects on monocytes, vascular endothelium, and vascular smooth muscle cells [10–12]. The present findings demonstrated that preincubation of monocytes with pioglitazone, a TZD, significantly reduced monocytic U937 adhesion to activated HUVEC under both static and flow conditions. Based on the results of flow cytometric analysis, pioglitazone did not have an effect on the expression levels of cell surface integrins in U937 cells. In parallel with this observation, recent reports have demonstrated that the surface expression levels of integrins do not exclusively modulate the adhesive interactions of leukocytes [13]. In the present experiments, we found a reduction of actin filament after pioglitazone treatment. Further, it has been reported that the actin cytoskeleton that is anchored to focal adhesion sites is critically important in monocyte adhesion to vascular endothelium [14], therefore, modulation of the cytoskeletal network leads to an increase or decrease of adhesive interactions. Pioglitazone significantly decreased the filamentous actin contents in U937 cells and the RhoA activity. This effect on RhoA inactivation and cytoskeletal modulation may show a novel intracellular mechanism by which pioglitazone inhibits monocyte adhesion. FAK is known to regulate cell adhesion and migration in various cell types, including non-adherent blood cells, by transferring signals to integrins at the cellular adhesion site [15]. Further, we showed that the phosphorylation of 925Y, which is reported to be associated with the Ras/mitogen-activated protein kinase pathway [16] was reduced by pioglitazone treatment. These data suggest that dephosphorylation at 925Y may be involved in the pioglitazone-mediated reduced adhesion of U937 cells. In contrast, the total amount of FAK and phosphorylation of FAK at tyrosine 397 was not affected by pioglitazone treatment. Interestingly, the PPARγ antagonist PGF2α failed to cancel the pioglitazone-mediated reduction of U937 cell adhesion, which implies that the observed phenomena occur independently of PPARγ agonistic stimulation. In agreement with our study, PPARγ-independent effects of PPARγ ligands were reported using TZDs [17]. Besides its activity as an agonist of PPARγ, pioglitazone may suppress the activation of RhoA GTPase. Careful examination in the future will be required to elucidate the responsible molecular mechanisms and other intracellular signaling important in cell adhesion. In summary, we demonstrated that pioglitazone, a novel antidiabetic agent, reduced IL-1β-induced monocyte adhesion to vascular endothelium, actin polymerization, and FAK activation. A reduction of RhoA GTPase activations may be involved in this process. Thus, in patients with diabetes, administration of pioglitazone is beneficial in reducing the serum level of glucose itself and may have clinical merits for modulating monocyte–endothelial interaction.

*Acknowledgements:* This study was supported in part by grants from the Ministry of Education, Science, Sports and Culture of Japan, and from the Ministry of Health, Labour and Welfare of Japan. We gratefully acknowledge the expert assistance of Noriko Nitta in working with the cell cultures.

## References

[1] Jiang, C., Ting, A.T. and Seed, B. (1998) Nature 391, 82–86.
[2] Ricote, M., Li, A.C., Willson, T.M., Kelly, C.J. and Glass, C.K. (1998) Nature 391, 79–82.
[3] Chawla, A., Barak, Y., Nagy, L., Liao, D., Tontonoz, P. and Evans, R.M. (2001) Nat. Med. 2001, 48–52.
[4] Yoshida, M. and Gimbrone Jr., M.A. (1997) Ann. NY Acad. Sci. 811, 493–497.
[5] Yoshida, M., Szente, B.E., Kiely, J.M., Rosenzweig, A. and Gimbrone Jr., M.A. (1998) J. Immunol. 161, 933–941.
[6] Kiely, J.M., Luscinskas, F.W. and Gimbrone Jr., M.A. (1999) Methods Mol. Biol. 96, 131–136.
[7] Yoshida, M., Sawada, T., Ishii, H., Gerszten, R.E., Rosenzweig, A., Gimbrone Jr., M., Yasukochi, Y. and Numano, F. (2001) Arterioscler. Thromb. Vasc. Biol. 21, 1165–1171.
[8] Li, S., Chen, B.P., Azuma, N., Hu, Y.L., Wu, S.Z., Sumpio, B.E., Shyy, J.Y. and Chien, S. (1999) J. Clin. Invest. 103, 1141–1150.
[9] Laufs, U. and Liao, J.K. (1998) J. Biol. Chem. 273, 24266–24271.
[10] Jiang, C., Ting, A.T. and Seed, B. (1998) Nature 391, 82–86.
[11] Murata, T., Hata, Y., Ishibashi, T., Kim, S., Hsueh, W.A., Law, R.E. and Hinton, D.R. (2001) Arch. Ophthalmol. 119, 709–717.
[12] Law, R.E., Goetze, S., Xi, X.P., Jackson, S., Kawano, Y., Demer, L., Fishbein, M.C., Meehan, W.P. and Hsueh, W.A. (2000) Circulation 101, 1311–1318.
[13] Kawakami, A., Tanaka, A., Nakajima, K., Shimokado, K. and Yoshida, M. (2002) Circ. Res. 91, 263–271.
[14] Takubo, T., Hino, M., Suzuki, K. and Tatsumi, N. (1999) Eur. J. Histochem. 43, 71–77.
[15] Zachary, I. and Rozengurt, E. (1992) Cell 71, 891–894.
[16] Schlaepfer, D.D., Hanks, S.K., Hunter, T. and van der Geer, P. (1994) Nature 372, 786–791.
[17] Palakurthi, S.S., Aktas, H., Grubissich, L.M., Mortensen, R.M. and Halperin, J.A. (2001) Cancer Res. 61, 6213–6218.

# Remnant Lipoprotein–Induced Smooth Muscle Cell Proliferation Involves Epidermal Growth Factor Receptor Transactivation

Akio Kawakami, MD; Akira Tanaka, MD; Tsuyoshi Chiba, PhD; Katsuyuki Nakajima, PhD; Kentaro Shimokado, MD; Masayuki Yoshida, MD

***Background***—Remnant lipoproteins (RLPs) have been shown to play a causative role during atherosclerosis. Furthermore, it is known that vascular smooth muscle cell (SMC) proliferation is crucial for the development of atherosclerosis and restenosis after percutaneous coronary intervention. We examined the direct effect of RLPs on the proliferation and signal transduction of SMCs.

***Methods and Results***—Incubation in the presence of RLPs (20 mg cholesterol per dL) for 48 hours induced rat aortic SMC proliferation (2.3-fold over medium alone). RLPs also induced the phosphorylation of epidermal growth factor (EGF) receptor in SMCs, which was followed by the activation of mitogen-activated protein kinases. Moreover, the activation of protein kinase C (PKC) as well as the shedding of membrane-bound soluble heparin-binding EGF-like growth factor (HB-EGF) was observed after RLP treatment of SMCs, whereas PKC inhibitors and metalloprotease inhibitors inhibited RLP-induced EGF receptor transactivation and HB-EGF shedding in SMCs. Furthermore, anti-HB-EGF neutralizing antibody inhibited RLP-induced EGF receptor transactivation. Phosphorylation of EGF receptor and HB-EGF shedding were also observed in the aortas of apolipoprotein E–knockout mice but not in those of C57BL6 mice.

***Conclusions***—These results suggest that RLPs transactivate EGF receptor via PKC and HB-EGF shedding from SMCs, resulting in SMC proliferation. (***Circulation.*** **2003;108:2679-2688.)**

**Key Words:** lipoproteins ■ muscle, smooth ■ signal transduction ■ atherosclerosis

Recent studies have demonstrated that serum remnant lipoproteins (RLPs) are atherogenic and may be a risk factor for ischemic heart disease, independent of LDL and HDL.[1] Our previous results have also suggested a causative role of RLPs in atherosclerosis.[2,3]

The proliferation of smooth muscle cells (SMCs) plays a critical role in intimal thickening of arteries associated with atherosclerosis or restenosis after percutaneous coronary intervention (PCI).[4] Several lipoproteins have been reported to induce the migration and proliferation of SMCs via activation of mitogen-activated protein kinase (MAPK), in which G protein–coupled receptor (GPCR)–dependent protein kinase C (PKC) activation was shown to be involved.[5,6] It is known that RLPs enter vessel walls, where they are easily taken up by macrophages via LDL receptors,[7] resulting in foam cell formation. However, the direct effects of RLPs on SMCs in media have not been fully elucidated, although we recently showed that RLPs directly stimulate porcine coronary artery SMC proliferation, independent of oxidative stress.[2] In line with those results, we examined the effects of RLPs on MAPK pathway and epidermal growth factor (EGF) receptor transactivation, along with the involvement of G protein–coupled receptor in rat aortic SMCs. Herein, we report for the first time that atherogenic RLPs from patients with hypertriglyceridemia stimulated rat SMC proliferation via heparin-binding EGF-like growth factor (HB-EGF) shedding and EGF receptor transactivation.

## Methods

### Cell Culture Reagents and Animals

SMCs were prepared from rat thoracic aortas and grown in DMEM (Sigma) supplemented with 10% FCS, 2 mmol/L L-glutamine, 100 μg/mL penicillin, and 100 U/mL streptomycin. Apolipoprotein E (apoE)–knockout male mice and C57BL6 male mice, each weighing between 29 and 32 g, were obtained from CLEA Japan (Tokyo, Japan) and Jackson Laboratory (Bar Harbor, Maine), respectively. All received water ad libitum and were fed a normal standard chow diet for 20 weeks, after which they were killed by heart puncture under diethyl-ether anesthesia. At 20 weeks of age, the apoE-knockout mice had already developed atherosclerotic lesions in the aorta. The aortas were carefully removed intact from the aortic arch to the iliac bifurcation and homogenized immediately for protein

Received July 30, 2002; de novo received May 20, 2003; revision received July 15, 2003; accepted July 16, 2003.

From the Departments of Medical Biochemistry (A.K., M.Y.) and Geriatrics and Vascular Medicine (A.K., T.C., K.S., M.Y.), Graduate School of Medicine, Tokyo Medical and Dental University; Department of Health and Nutrition (A.T.), College of Human Environmental Studies, Kanto-gakuin University; and Japan Immunoresearch Laboratories (K.N.), Takasaki, Japan.

Correspondence to Masayuki Yoshida, MD, Department of Medical Biochemistry, Graduate School of Medicine, Tokyo Medical and Dental University, 1-5-45, Yushima, Building D-256, Bunkyo-ku, Tokyo 113-8519, Japan. E-mail masa.vasc@tmd.ac.jp



*Circulation* is available at http://www.circulationaha.org

DOI: 10.1161/01.CIR.0000093278.75565.87

extraction. All animal procedures were approved by the Institutional Animal Care Committee of Tokyo Medical and Dental University (approval No. 0010209) and conducted according to Guidelines for Animal Experimentation at Tokyo Medical and Dental University.

The antibodies used in the present study were as follows: rabbit anti-EGF receptor polyclonal antibody, rabbit anti-phospho-EGF receptor polyclonal antibody (Santa Cruz Biotechnology, Santa Cruz, Calif), rabbit anti-MEK1/2 polyclonal antibody, rabbit anti-phospho-MEK1/2 polyclonal antibody, rabbit anti-ERK1/2 polyclonal antibody, rabbit anti-phospho-ERK1/2 polyclonal antibody, mouse anti-PKC$\alpha$, $\beta$, $\delta$, $\epsilon$, $\gamma$, $\lambda$, $\eta$, $\iota$, and $\theta$ monoclonal antibodies (New England Biolabs, Beverly, Mass), and anti-phosphotyrosine monoclonal antibody (pY20) (Cell Signaling, Beverly, Mass). A neutralizing goat anti-HB-EGF polyclonal IgG was obtained from Oncogene, and its specific inhibition was confirmed with rat SMCs stimulated by rat recombinant HB-EGF (kindly provided by Dr Shigeki Higashiyama, Ehime University, Matsuyama, Japan).

## Lipoprotein Preparation

EDTA plasma was obtained from 20 patients with hypertriglyceridemia who showed elevated fasting serum RLP concentrations (>7.5 mg cholesterol per dL) 4 hours after eating breakfast.[3] They had no cardiovascular diseases or diabetes and had not received cardiovascular medicine or antioxidants. RLPs were isolated from plasma samples using an RLP-C Kit (Japan Immunoresearch Laboratories), as described previously.[8] The prepared RLPs were found to mainly consist of VLDL remnants and a few CM remnants.[3] Lipoproteins and lipids were dialyzed overnight against 5 L of PBS containing 50 $\mu$mol/L EDTA (pH 7.4) and then sterilized using a 0.22-$\mu$m filter unit (Millipore). RLP lipid fractions were extracted using chloroform/methanol and then dried under $N_2$ gas. Trypsinized RLPs (devoid of immunochemically detectable apoE) were prepared as described previously.[9] Endotoxin levels in the lipoprotein and lipid preparations, measured using a Limulus test assay kit (Wako), were less than 0.03 EU/mL.

## Cell Proliferation Assay

Subcultured SMCs (passages 2 through 7) were seeded into 96-well microplates ($3\times10^3$ cells/well) or 35-mm dishes ($2\times10^4$ cells/dish). The culture medium was changed to DMEM supplemented with 1.0% FCS at 24 hours after seeding, and SMCs were made quiescent by incubating for 3 days, after which they were incubated with RLPs at the indicated concentrations or medium alone for the indicated hours. At the end of incubation, the incorporation of 5-bromo-2'-deoxyuridine (BrdU) into SMCs was examined using a microplate reader (CytoFlourII, Perceptive Biosystem).[10] In parallel with the BrdU incorporation assay, SMCs were also stained with 4',6-Diamidino-2-phenylindole, dihydrochloride (DAPI) (200 ng/mL) and viable cells were counted at the required time point using a hemacytometer.

## Immunoprecipitation and Immunoblotting

A cell lysate from homogenized aorta samples was immunoprecipitated with anti-EGF receptor antibody. Fifty microliters of anti-rabbit IgG affinity gel (ICN Biomedicals) was then added for an additional

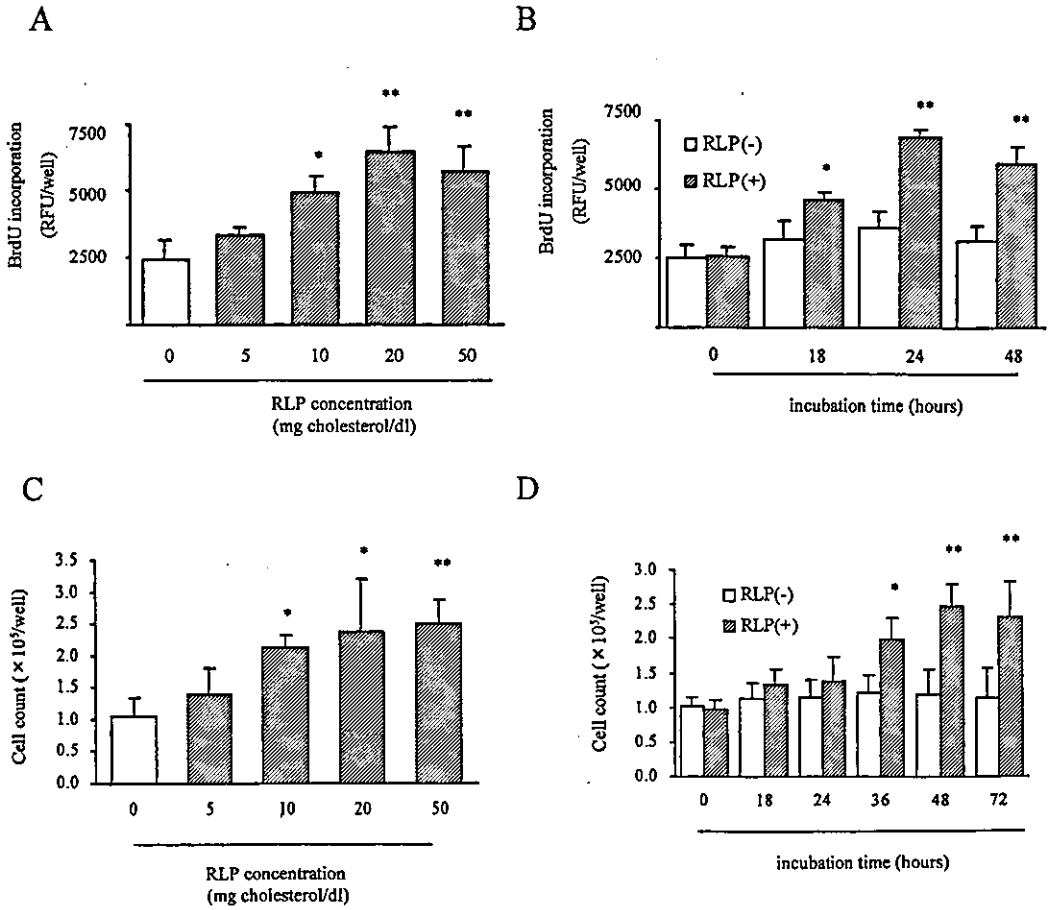


Figure 1. Effects of RLPs on SMC DNA synthesis and proliferation. A and C, SMCs were incubated in the presence of increasing concentrations of RLPs for up to 24 (A) or 48 (C) hours, and then a BrdU incorporation assay was carried out (n=6) (A) or the number of SMCs was counted using a hemacytometer (n=6) (C). *$P$<0.05, **$P$<0.01 vs 0 mg cholesterol per dL. B and D, SMCs were incubated in the absence (−) or presence (+) of RLPs (20 mg cholesterol per dL) for the indicated hours, and then a BrdU incorporation assay was carried out (n=6) (B) or the number of SMCs was counted using a hemacytometer (n=6) (D). *$P$<0.05,**$P$<0.01 vs 0 hours.

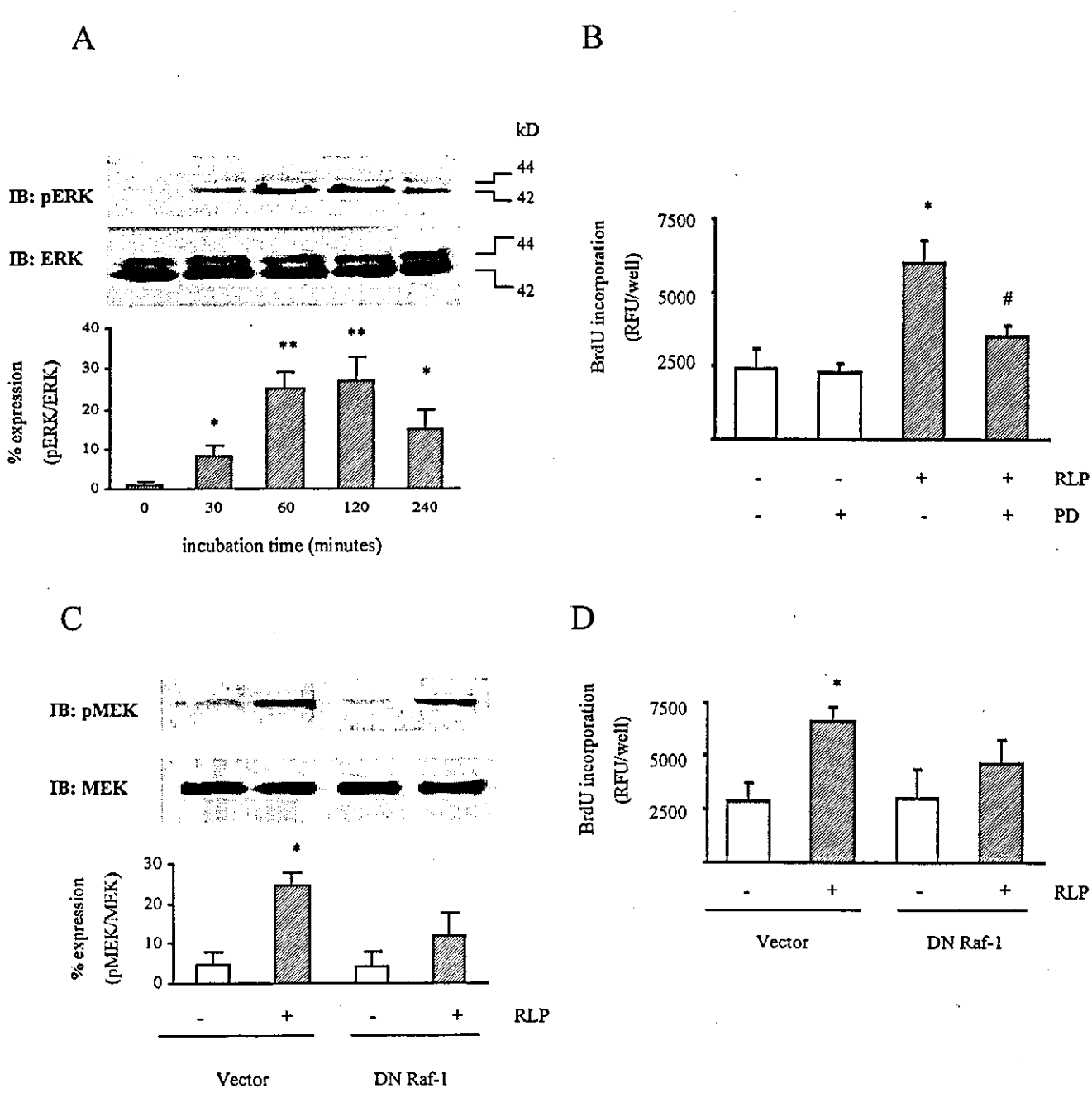


**Figure 2.** Involvement of MAPK in RLP-induced SMC proliferation. A, SMCs were incubated in the presence of RLPs (20 mg cholesterol per dL) for the indicated minutes before Western blotting (blots are representative of 6 separate experiments). *$P<0.05$,**$P<0.01$ vs 0 minutes. B, SMCs were preincubated in the absence (−) or presence (+) of PD98059 (PD) (50 μmol/L) for 4 hours and then incubated in the absence (−) or presence (+) of RLPs (20 mg cholesterol per dL) for 24 hours before a BrdU incorporation assay (n=4). *$P<0.01$ vs RLP (−)/PD (−), #$P<0.01$ vs RLP (+)/PD (−). C and D, SMCs were transfected with DN Raf-1 in pUSEamp (DN Raf-1) or pUSEamp alone (vector) and then incubated in the absence (−) or presence (+) of RLPs (20 mg cholesterol per dL) for 120 minutes (C) or 24 hours (D) before Western blotting (blots are representative of 3 separate experiments) (C) or a BrdU incorporation assay (n=3) (D). *$P<0.05$ vs RLP (−).

60 minutes, after which the immune complexes were collected and resuspended in SDS-PAGE sample buffer. SMCs were also incubated with RLPs (20 mg cholesterol per dL) for the indicated minutes, after which the membrane fractions and total cell lysates of SMCs were collected, as described previously.[3] An equal amount of protein (10 μg) from each condition was subjected to SDS-PAGE. Immunoblots were developed with ECL plus (Amersham Pharmacia Biotech).

## SMC Transfection

Quiescent SMCs were transfected with dominant-negative (DN) Raf-1 cDNA in pUSEamp (Upstate Biotechnology)[11] or in pUSEamp alone using a calcium phosphate method. To access the transfection efficiency, pCxEGFP[12] was cotransfected and green fluorescent protein–positive SMCs were detected using fluorescent microscopy (IX70) (Olympus). The estimated transfection efficiency based on green fluorescent protein staining was from 26% to 29%. Transfected SMCs at 24 hours after transfection were used for cell proliferation and Western blotting assays.

## Statistical Analysis

Results are presented as mean±SEM. Data were analyzed using ANOVA, with $P<0.05$ considered significant.

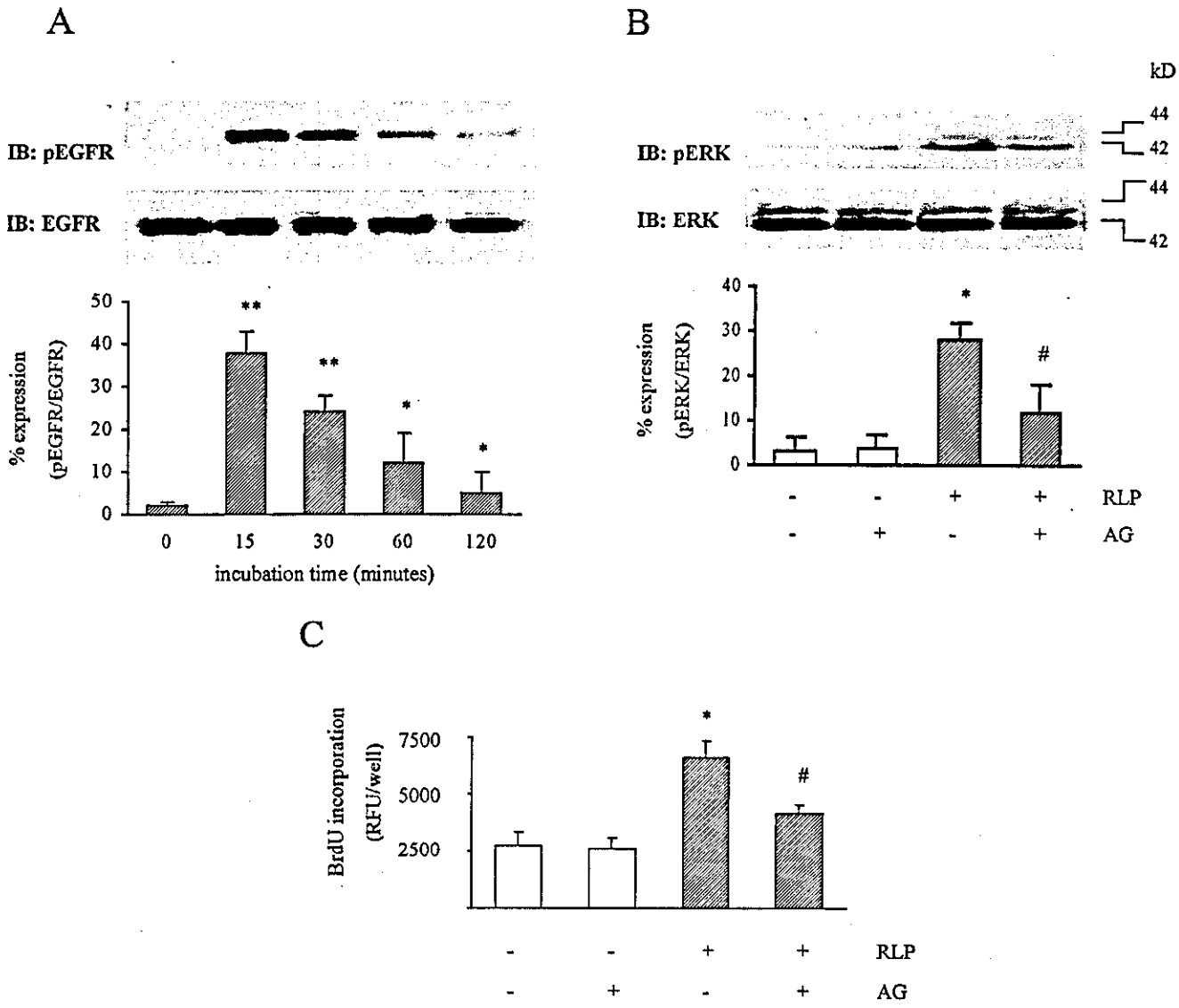


**Figure 3.** Involvement of EGF receptor transactivation in RLP-induced SMC proliferation. A, SMCs were incubated in the presence of RLPs (20 mg cholesterol per dL) for the indicated minutes before Western blotting (blots are representative of 3 separate experiments). *$P<0.05$,**$P<0.01$ vs 0 minutes. B and C, SMCs were preincubated in the absence (−) or presence (+) of AG1478 (AG) (1 μmol/L) for 30 minutes and then incubated with RLPs (20 mg cholesterol per dL) for 120 minutes (B) or 24 hours (C) before Western blotting (blots are representative of 3 separate experiments) (B) or a BrdU incorporation assay (n=4) (C). *$P<0.05$ vs RLP (−)/AG (−), #$P<0.05$ vs RLP (+)/AG (−).

## Results

### RLPs Induce SMC Proliferation

First, we examined the effects of RLPs on rat aortic SMC proliferation. When SMCs were incubated in the presence of RLPs for 24 hours, BrdU incorporation into SMCs was significantly increased at pathophysiological concentrations (>7.5 mg cholesterol per dL) in a dose-dependent manner (Figure 1A), and RLP-induced BrdU incorporation reached a peak after 24 hours of incubation (Figure 1B). The total number of SMCs simultaneously counted under the same conditions increased in a dose- and time-dependent manner (Figures 1C and 1D). In the following experiments, we chose to incubate SMCs with RLPs at 20 mg cholesterol per dL for 24 hours, unless otherwise indicated.

### Involvement of MAPK Signal Transduction in RLP-Induced SMC Proliferation

Next, activation of MAPK pathway in RLP-treated SMCs was examined. Phosphorylated ERK1/2 increased after treatment with RLPs (Figure 2A). RLPs induced a sequential activation of Raf-1-MEK1/2-ERK1/2 (data not shown). Pretreatment with PD98059 (Calbiochem), a specific MEK1 inhibitor, significantly inhibited RLP-induced SMC BrdU incorporation (Figure 2B). Furthermore, the transfection of DN Raf-1 reduced RLP-induced MEK1/2 activation and SMC BrdU incorporation (Figures 2C and 2D).

### RLP-Induced EGF Receptor Transactivation in SMCs

We then examined activation of the EGF receptor in RLP-treated SMCs. As shown in Figure 3A, the receptor was